

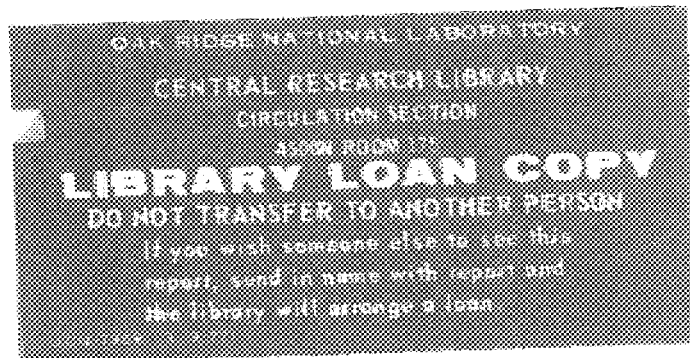
ornl

**OAK RIDGE
NATIONAL
LABORATORY**

MARTIN MARIETTA

Nonlinear Maps with Competitive Interactions: Fixed-Points, Bifurcations, and Chaotic Attractors

D. F. Scollan
Y. Y. Azmy
V. Protopopescu



OPERATED BY
MARTIN MARIETTA ENERGY SYSTEMS, INC.
FOR THE UNITED STATES
DEPARTMENT OF ENERGY

This report has been reproduced directly from the best available copy.

Available to DOE and DOE contractors from the Office of Scientific and Technical Information, P.O. Box 62, Oak Ridge, TN 37831; also available from (615) 576-8401, FTB 6068401.

Available to the public from the National Technical Information Service, U.S. Department of Commerce, 5285 Port Royal Rd., Springfield, VA 22161.
NTIS price and availability statements are given on the inside cover.

This report was prepared as an account of work sponsored by the United States Government. Certain rights are reserved by the Government. Reproduction for Government use is authorized. It is understood that any copyright appearing hereon does not constitute an acknowledgment of the Government's ownership of the material. It is also understood that any copyright appearing hereon does not constitute an acknowledgment of the Government's sponsorship of the work. This report is available to the public through the National Technical Information Service, U.S. Department of Commerce, 5285 Port Royal Rd., Springfield, VA 22161. NTIS price and availability statements are given on the inside cover.

ORNL/TM-11315

Engineering Physics and Mathematics

**Nonlinear Maps with Competitive Interactions:
Fixed-Points, Bifurcations, and Chaotic Attractors**

D. F. Scollan*, Y. Y. Azmy, and V. Protopopescu

DATE PUBLISHED — SEPTEMBER 1989

*Pennsylvania State University

Prepared by the
OAK RIDGE NATIONAL LABORATORY
Oak Ridge, Tennessee 37831
operated by
MARTIN MARIETTA ENERGY SYSTEMS, INC.
for the
U.S. DEPARTMENT OF ENERGY
under contract DE-AC05-84OR21400



3 4456 0318984 0

CONTENTS

ACKNOWLEDGMENTS	v
ABSTRACT	vii
1. INTRODUCTION	1
2. ANALYTICAL INVESTIGATION OF A SPECIAL TWO SPECIES SYSTEM	4
2.1 INTRODUCTION	4
2.2 ANALYTICAL DETERMINATION OF THE FIXED AND PERIOD- TWO SOLUTIONS	4
2.3 GENERAL CONSTRAINTS ON THE PERIODIC SOLUTIONS	5
2.4 LINEAR STABILITY OF THE FIXED POINTS	9
2.5 DETERMINATION OF THE PARAMETRIC REGIONS WHICH YIELD STABLE PERIODIC SOLUTIONS	10
2.6 ANOMALOUS NUMERICAL SOLUTIONS	13
3. ANALYSIS OF A GENERALIZED TWO-SPECIES SYSTEM	19
3.1 INTRODUCTION	19
3.2 DETERMINATION OF THE FIXED POINTS	19
3.3 LINEAR STABILITY OF THE FIXED POINTS	20
3.4 NUMERICAL ANALYSIS OF THE BEHAVIOR OF SYSTEM (3-1-1) FOR VARIOUS VALUES OF THE PARAMETER A	21
3.5 THE EVOLUTION OF THE INSTABILITY	21
3.6 CONCLUSIONS	35
4. NUMERICAL ANALYSIS OF SYSTEM (1-1-4)	36
4.1 INTRODUCTION	36
4.2 DESCRIPTION OF THE COMPUTER PROGRAM	36
4.3 NUMERICAL ANALYSIS OF SYSTEM (1-1-4) FOR BILINEAR ATTRITION AND LOW SELF-REPRESSION	36
4.4 ANALYSIS OF SYSTEM (1-1-4) WITH LINEAR ATTRITION	40
4.5 CONCLUSIONS FOR THE ANALYSIS OF SYSTEM (1-1-4)	41
5. NUMERICAL ANALYSIS OF SYSTEM (1-1-1)	46
5.1 INTRODUCTION	46
5.2 DESCRIPTIONS OF THE PROGRAMS	46
5.3 ONE-SPECIES DYNAMICS	46

5.4 A COMPARISON OF SYSTEM (1-1-4) AND SYSTEM (1-1-1) DYNAMICS	47
5.5 CONCLUSIONS	47
6. CALCULATION OF THE CORRELATION DIMENSION OF THE CHAOTIC ATTRACTOR	58
6.1 INTRODUCTION	58
6.2 ESTIMATION OF THE CORRELATION DIMENSION	58
6.3 RESULTS	59
6.4 A STATISTICAL ANALYSIS	59
APPENDIX 1	62
REFERENCES	66

ACKNOWLEDGMENTS

This work has been partly sponsored by DARPA under contract number 1868-A037-A1 with Martin Marietta Energy Systems, Inc., which is under contract number DE-AC05-84OR21400 with the U.S. Department of Energy. The main part of this work has been completed during D. F. Scollan's ORSERS internship at the Oak Ridge National Laboratory supported by the Oak Ridge Associated Universities.

ABSTRACT

We examine several aspects of the dynamical behavior of competitive systems modeled by nonlinear maps. In the second chapter of this report, we analytically investigate some features of special cases of such maps, and we use the symbolic manipulator MACSYMA to derive expressions for the linearized systems' eigenvalues. These enable us to determine the linear stability of some of the fixed and periodic points of these maps, and in some cases, yield the regions of attraction in phase space.

In Chapters 3-5 we extend the analysis to a more general form of competitive systems. The two-species one-index system and the one-species two-index map are numerically explored in search for interesting bifurcation and/or chaotic regimes over a large range of parameters. We will show that system (1-1-4) with linear attrition displays stable, interesting behavior for a large region of parameter space even if the quadratic self-repression is taken very small. We will also show that small quadratic self-repression combined with bilinear attrition generally results in steady-state solutions with one species zero or in unbounded iterates.

In Chapter 6, we describe the method used to obtain an approximate estimate of the correlation dimensions of the chaotic attractor presented in Chapter 3. We also propose a new method to evaluate the correlation dimension of a chaotic attractor using statistical analysis methods.

1. INTRODUCTION

A two-dimensional finite difference map has recently been proposed as a discrete time- and space-dependent model for competitive systems.¹ This map was derived from a time- and space-dependent partial differential equation (PDE) model of combat.² The two-species, two-index version of the finite difference system has the following form in one space dimension:

$$\begin{aligned}
 \left[\frac{u_i^{n+1,m} - u_i^{n,m}}{\tau} \right] &= \left[\frac{D_i^{m+1}(u_i^{n,m+1} - u_i^{n,m}) - D_i^m(u_i^{n,m} - u_i^{n,m-1})}{\delta^2} \right] \\
 &- (1 - W_i^{m+1})C_i^{m+1} \left[\frac{u_i^{n,m+1} - u_i^{n,m}}{\delta} \right] - W_i^m C_i^m \left[\frac{u_i^{n,m} - u_i^{n,m-1}}{\delta} \right] \\
 &- \sum_{j,k=1}^2 \left[a_{ijk} u_j^{n,m} u_k^{n,m} + b_{ij} u_j^{n,m} \right] + \left[\frac{S_i^m + S_i^{m+1}}{2} \right] \\
 &- \sum_{j=1}^2 \left\{ \sum_{\substack{l=1, \\ l \neq m}}^M \phi_{ij} u_i^{n,m} u_j^{n,l} + \sum_{\substack{l=1, \\ l \neq m}}^M \psi_{ij} u_j^{n,l} \right\}, \quad i = 1, 2.
 \end{aligned} \tag{1-1-1}$$

The variables u_1 and u_2 represent the area densities of the two forces (species) at a given node, m , and at a given iteration (time), n . The term on the left-hand side of Eq. (1-1-1) models the variation of the densities of the species with time. The first bracketed term on the right-hand side of Eq. (1-1-1) represents diffusion effects. The second and third bracketed terms model convective motion (advance and retreat) of the two forces. The fourth bracketed term models self-repression, resupply, and local attrition effects. The fifth term allows for the existence of autonomous sources. The sixth term models nonlocal attrition, whose first part is analogous to the area fire term and second part to the aimed fire term in Lanchester's seminal ordinary differential equation (ODE) model of combat.^{3,4} The functions ϕ and ψ modulate the effect of these terms over distance. The nonlocal terms were not present in the previous study¹ of system (1-1-1). However, their analogies appear in the PDE model and we shall include them in future studies of system (1-1-1). The form of system (1-1-1) is complete with the specification of the initial conditions

$$u_i^{n=0,m} = u_i^{0,m}, \quad m = 0, \dots, M, \quad i = 1, 2 \tag{1-1-2}$$

and the boundary conditions

$$\frac{\alpha_i^k}{2\delta} \left[u_i^{n,k+1} - u_i^{n,k-1} \right] + \beta_i^k u_i^{n,k} = e_i^k, \quad k = 0, M, \quad i = 1, 2. \tag{1-1-3}$$

For a full description of the form and derivation of this map, see Reference 1.

A previous analytical and numerical analysis of system (1-1-1), largely centered on the dynamics of the one species (two noninteracting species) version, has been conducted.¹ The full-blown system (1-1-1) is analytically intractable. Furthermore,

the large number of parameters makes even a numerical investigation extremely difficult. The purpose of this paper is to provide more insight into the dynamics of system (1-1-1). To this end, we analyze the following simplified, space-independent version of this system:

$$\begin{aligned}x_{n+1} &= A_1x_n(1 - B_1x_n - C_1y_n) - D_1y_n + E_1 \\y_{n+1} &= A_2y_n(1 - B_2y_n - C_2x_n) - D_2x_n + E_2\end{aligned}\tag{1-1-4}$$

Species u_1 and u_2 have been renamed as species x and y . Diffusion and convection have been removed in this model, as well as some local terms. Those that remain have the following interpretations in the context of combat modeling:

Expression	Interpretation
A_1x, A_2y	For $A_1, A_2 \geq 1$, these terms model resupply (reinforcement). If A_1 or A_2 is taken less than or equal to one, and no source terms are present, then one force will necessarily be annihilated.
E_1, E_2	For $E_1, E_2 \geq 0$, they model autonomous sources.
D_1y, D_2x	For $D_1, D_2 \geq 0$, these terms model aimed fire. Their form assumes that all members of the targeted force are visible to and within range of the firing force, and that once a member of the targeted force is killed, fire is concentrated on the remaining combatants. ⁴ Fire is assumed proportional to the force levels (the values of x and y). As the number of the force firing their weapons decreases, the effectiveness of this term decreases. The Lanchester ODE system using linear attrition in both species was found to model well the battle of Iwo Jima. ⁴
C_1xy, C_2xy	For $C_1, C_2 \geq 0$, these terms model area fire. Unlike aimed fire, these terms model fire targeted into a region, rather than at a specific combatant. The effectiveness of this kind of fire increases as the density of the targeted force in the area increases and as the amount of fire (again assumed proportional to the size of the firing force) increases. Examples of area fire situations are artillery fire and fire directed at hidden guerilla forces. ⁴ Also, these attrition terms have some support from their similar use in predator-prey models. ^{4,5}
B_1x^2, B_2y^2	For $B_1, B_2 \geq 0$, they model self-repressing effects (such as a loss of efficiency) due to crowding, saturation, etc. ² It would seem natural that such effects should be small compared to attrition effects. We include these terms for completeness, because as will be shown, the dynamics mapping (1-1-4) depends highly on the presence or absence of these terms. We will especially want to determine the behavior of system (1-1-4) for small, and thus more plausible, self-repression effects.

While we have given the interpretation of the terms in the context of combat modeling, we certainly do not hold that the very simplistic system (1-1-4) should be construed as a model of combat. No attempt is made here to derive conclusions about the dynamics of forces in combat from the analysis of this system. Rather, we analyze this system in order to provide a heuristic understanding of the dynamics of system (1-1-1). Furthermore, the dynamics of system (1-1-4) can be considered interesting in its own right.

2. ANALYTICAL INVESTIGATION OF A SPECIAL TWO SPECIES SYSTEM

2.1 INTRODUCTION

This chapter summarizes the dynamics of the two species logistic map:

$$\begin{aligned}x_{n+1} &= A_1 x_n \left(1 - \frac{x_n}{2} - \frac{y_n}{2}\right) \\y_{n+1} &= A_2 y_n \left(1 - \frac{x_n}{2} - \frac{y_n}{2}\right), \quad n = 0, 1, 2, \dots\end{aligned}\tag{2-1-1}$$

This map can be viewed as a model of the dynamics of two competing species. The linear terms represent resupply, the quadratic terms self-repression, and the bilinear terms attrition.

Single⁶ and double⁷ precision computer programs written in VAX FORTRAN⁸ are used to simulate the map. Bifurcation diagrams are generated using DISSPLA⁹ graphic library routines.

The fixed points and period two solutions for Eqs. (2-1-1) are determined analytically using MACSYMA.¹⁰ A discussion of the results is in Section 2.2 and the MACSYMA output is listed in Appendix 1.

In Section 2.3, we prove that all periodic solutions to Eqs. (2-1-1) must have at least one component equal to zero, except for the degenerate case $A_1 = A_2$, which has infinitely many parameterized periodic solutions. Thus, for the nondegenerate case, Eqs. (2-1-1) asymptotically approach a single species logistic map.

Sections 2.4 and 2.5 discuss the linear stability of the fixed and periodic solutions of Eqs. (2-1-1), respectively. These sections give necessary constraints, in terms of A_1 and A_2 , for the linear stability of the solutions.

Section 2.6 is motivated by the numerical analysis of Eqs. (2-1-1) with $A_2 = 3$, which shows iterates in a stable or nearly stable 2-cycle closely straddling a fixed point for a large range of parameter values. However, it is shown analytically that no 2-cycle exists in the region. A plausible explanation based on computer storage of a finite number of significant digits is given.

2.2 ANALYTICAL DETERMINATION OF THE FIXED AND PERIOD-TWO SOLUTIONS

The fixed points of the map represented by Eqs. (2-1-1) satisfy

$$\begin{aligned}\bar{x} &= A_1 \bar{x} \left(1 - \frac{\bar{x}}{2} - \frac{\bar{y}}{2}\right) \\ \bar{y} &= A_2 \bar{y} \left(1 - \frac{\bar{x}}{2} - \frac{\bar{y}}{2}\right)\end{aligned}\tag{2-2-1}$$

The origin

$$\bar{x} = 0, \bar{y} = 0\tag{2-2-2a}$$

is a trivial fixed point. The fixed point

$$\bar{x} = 0, \bar{y} = 2 \left(1 - \frac{1}{A_2} \right) \quad (2-2-2b)$$

exists for all nonvanishing values of A_2 . Similarly, the fixed point

$$\bar{x} = 2 \left(1 - \frac{1}{A_1} \right), \bar{y} = 0 \quad (2-2-2c)$$

exists for all $A_1 \neq 0$. Eqs. (2-2-1) also have a one-parameter family of solutions

$$\bar{y} = 2 \left(1 - \frac{1}{A} \right) - \bar{x} \quad (2-2-2d)$$

if $A_1 = A_2 = A \neq 0$.

We used the symbolic manipulator MACSYMA¹⁰ to calculate the fixed points of Eqs. (2-2-1) as functions of the parameters A_1 and A_2 . MACSYMA found all the above solutions except (2-2-2d). The MACSYMA routine did produce (2-2-2d) when A_1 was explicitly set equal to A_2 . These results, along with the MACSYMA routine's period-two solutions, are included in Appendix 1.

2.3 GENERAL CONSTRAINTS ON THE PERIODIC SOLUTIONS

In this section, we prove that periodic orbits of Eqs. (2-1-1) must have one component zero, except in the degenerate case, $A_1 = A_2$. Thus for $A_1 \neq A_2$, stable periodic trajectories of Eqs. (2-1-1) reduce asymptotically to those of a single component logistic map (see Figures 1 and 2).

Proof:

Equations (2-1-1) can be written as a system of functions:

$$\begin{aligned} f_1(x, y) &= A_1 x \left(1 - \frac{x}{2} - \frac{y}{2} \right) \\ f_2(x, y) &= A_2 y \left(1 - \frac{x}{2} - \frac{y}{2} \right) \end{aligned} \quad (2-3-1)$$

The first composition yields

$$\begin{aligned} f_1^2(x, y) &= A_1 f_1 \left(1 - \frac{f_1}{2} - \frac{f_2}{2} \right) \\ f_2^2(x, y) &= A_2 f_2 \left(1 - \frac{f_1}{2} - \frac{f_2}{2} \right) \end{aligned}$$

and the second composition yields

$$f_1^3(x, y) = A_1 f_1^2 \left(1 - \frac{f_1^2}{2} - \frac{f_2^2}{2} \right) = A_1^2 f_1 \left(1 - \frac{f_1}{2} - \frac{f_2}{2} \right) \left(1 - \frac{f_1^2}{2} - \frac{f_2^2}{2} \right)$$

and similarly for $f_2^3(x, y)$.

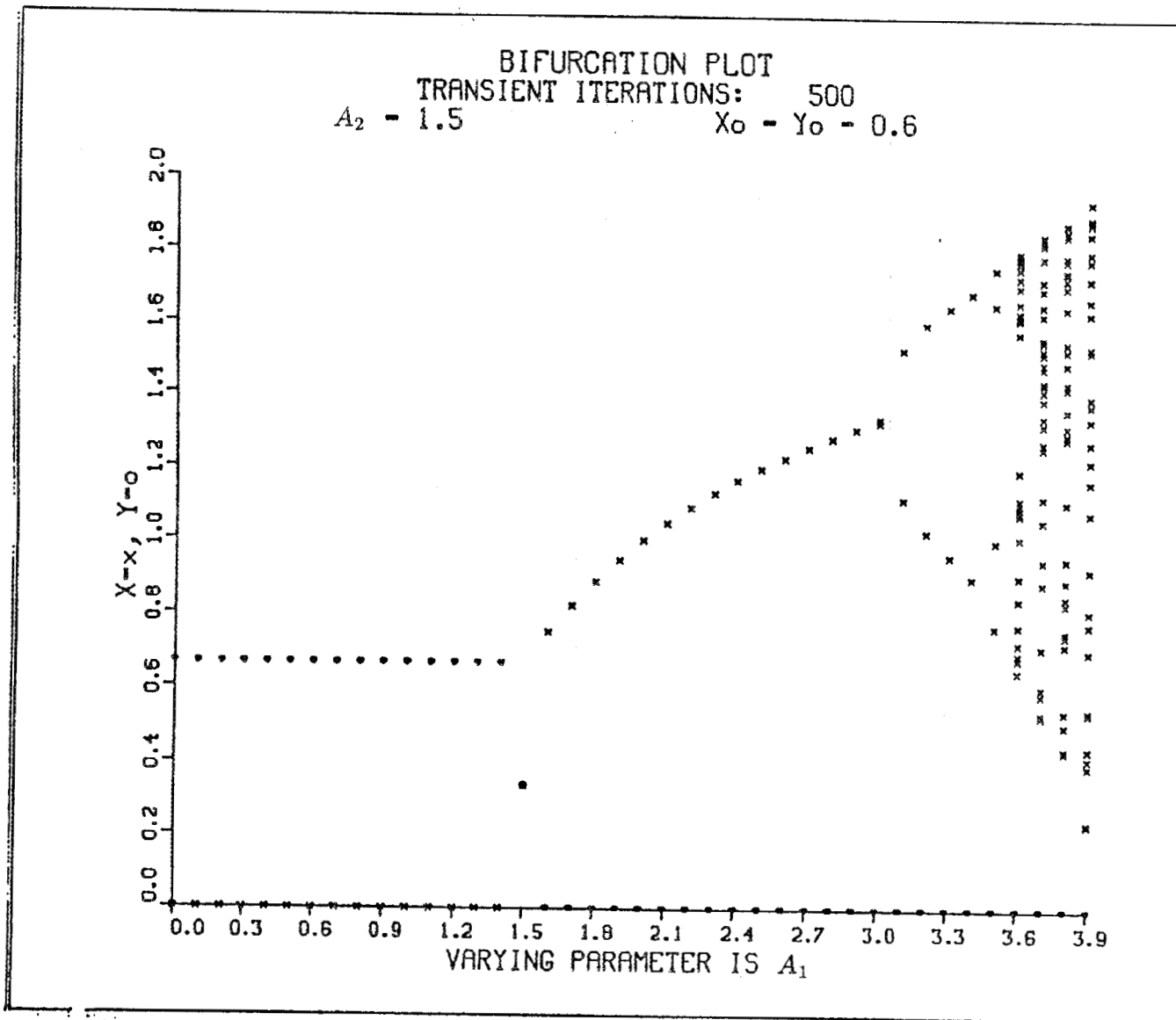


Figure 1. Bifurcation diagram for map (2-1-1). Note that one species always becomes equal to zero after sufficient iterations, except in the degenerate case.

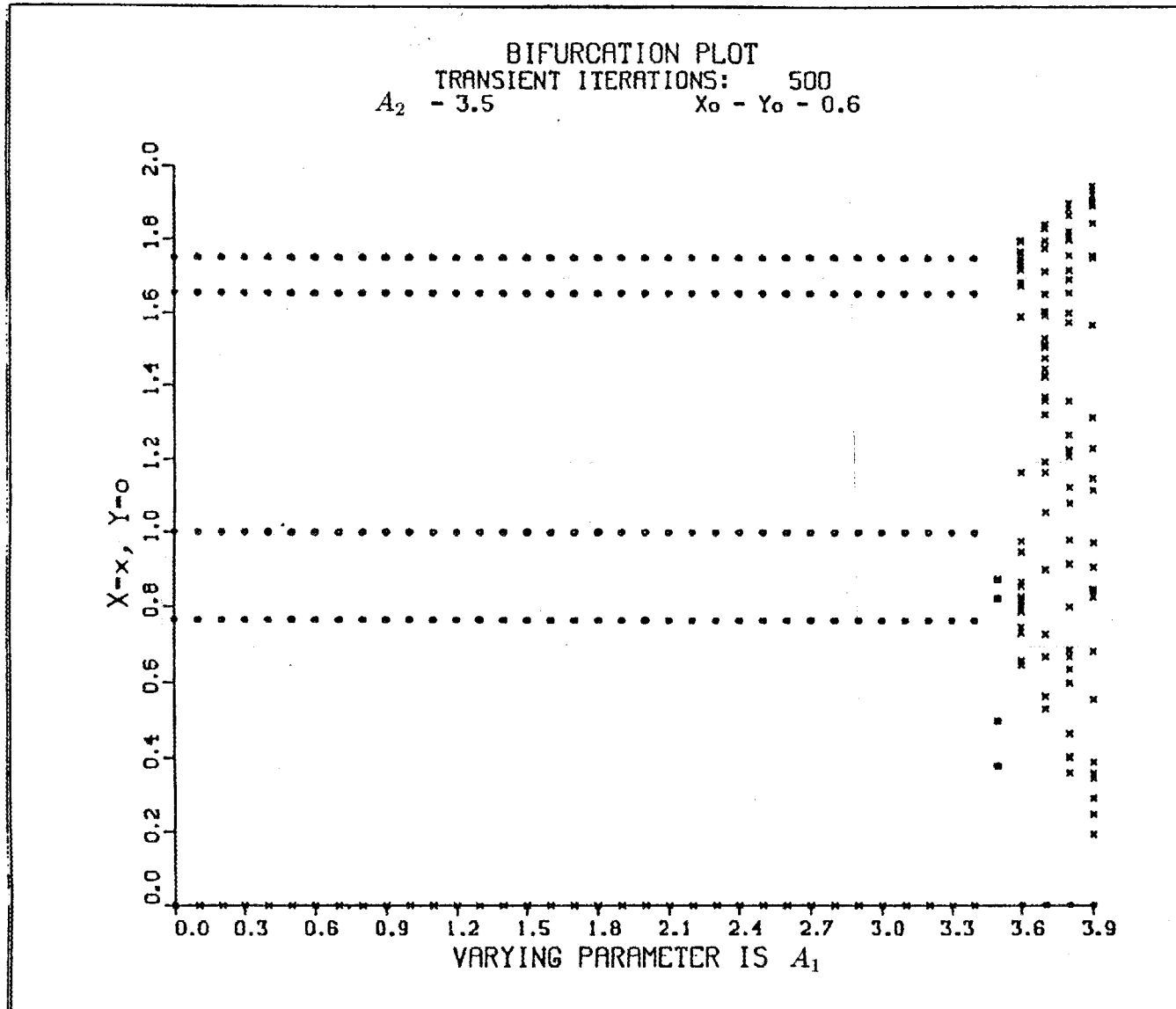


Figure 2. Bifurcation diagram for map (2-1-1). A second example of the steady state behavior of the map.

Suppose the n th composition yields

$$\begin{aligned} f_1^n(x, y) &= A_1^{n-1} f_1 \prod_{i=1}^{n-1} \left(1 - \frac{f_1^i}{2} - \frac{f_2^i}{2} \right) \\ f_2^n(x, y) &= A_2^{n-1} f_2 \prod_{i=1}^{n-1} \left(1 - \frac{f_1^i}{2} - \frac{f_2^i}{2} \right) \end{aligned} \quad (2-3-2)$$

for some $n > 1$. By showing Eqs. (2-3-2) holds also for the case $n + 1$, Eqs. (2-3-2) will be proven by mathematical induction for all $n > 1$. The $n + 1$ composition of Eqs. (2-1-1) is

$$\begin{aligned} f_1^n(f_1, f_2) &= A_1^{n-1} f_1^2 \prod_{i=1}^{n-1} \left(1 - \frac{f_1^{i+1}}{2} - \frac{f_2^{i+1}}{2} \right) \\ &= A_1^n f_1 \left(1 - \frac{f_1}{2} - \frac{f_2}{2} \right) \prod_{i=1}^{n-1} \left(1 - \frac{f_1^{i+1}}{2} - \frac{f_2^{i+1}}{2} \right) \end{aligned}$$

which becomes

$$f_1^{n+1}(x, y) = A_1^n f_1 \prod_{i=1}^n \left(1 - \frac{f_1^i}{2} - \frac{f_2^i}{2} \right)$$

and similarly for f_2^{n+1} , which is just the case $n = n + 1$ of Eqs. (2-3-2). Thus, Eqs. (2-3-2) is valid for all $n > 1$. Solving for the period- n solutions and using the definitions of f_1^n and f_2^n gives

$$\begin{aligned} x &= A_1^n x \left(1 - \frac{x}{2} - \frac{y}{2} \right) \prod_{i=1}^{n-1} \left(1 - \frac{f_1^i}{2} - \frac{f_2^i}{2} \right) \\ y &= A_2^n y \left(1 - \frac{x}{2} - \frac{y}{2} \right) \prod_{i=1}^{n-1} \left(1 - \frac{f_1^i}{2} - \frac{f_2^i}{2} \right) . \end{aligned} \quad (2-3-3)$$

We will assume the system (2-1-1) has periodic solutions of period- n given by Eqs. (2-3-3) with neither x nor y zero, and show a contradiction develops. For this case, Eqs. (2-3-2) become

$$\begin{aligned} \frac{1}{A_1^n} &= \left(1 - \frac{x}{2} - \frac{y}{2} \right) \prod_{i=1}^{n-1} \left(1 - \frac{f_1^i}{2} - \frac{f_2^i}{2} \right) \\ \frac{1}{A_2^n} &= \left(1 - \frac{x}{2} - \frac{y}{2} \right) \prod_{i=1}^{n-1} \left(1 - \frac{f_1^i}{2} - \frac{f_2^i}{2} \right) , \quad n > 1 , \end{aligned} \quad (2-3-4)$$

which is a contradiction unless $A_1 = A_2$, the degenerate case. While Eqs. (2-3-2)–(2-3-4) hold only for $n > 1$ because of the upper limit on the \prod operator, the conclusion holds for fixed points, $n = 1$, as we have shown in Section 2.2.

Therefore, Eqs. (1-3-1) cannot have periodic solutions with both components different from zero unless $A_1 = A_2$. Furthermore, when $A_1 = A_2$, Eqs. (2-3-4) reduces to one equation in two unknowns. This implies there will exist infinitely many parameterized periodic solutions.

2.4 LINEAR STABILITY OF THE FIXED POINTS

In this section, a linear stability analysis of the fixed points of Eqs. (2-1-1) is performed. Sufficient constraints on A_1 and A_2 are derived to insure linear stability of the fixed points, Eqs. (2-2-2). Then it is shown that the stability of all fixed points of the map (2-1-1) with $A_1 = \{1, 3\}$ or $A_2 = \{1, 3\}$ cannot be determined by linear analysis. Furthermore, in the next section, we show that for Eqs. (2-1-1) in general, the stability of periodic orbits of period two or more cannot be determined by linear analysis either.

Rewriting Eqs. (2-1-1) in vector form,

$$\underline{F} = \begin{bmatrix} f_1(x, y) = A_1 x - \frac{A_1}{2} x^2 - \frac{A_1}{2} xy \\ f_2(x, y) = A_2 y - \frac{A_2}{2} y^2 - \frac{A_2}{2} xy \end{bmatrix}. \quad (2-4-1)$$

The Jacobian of \underline{F} is given by

$$J\underline{F} = \begin{bmatrix} A_1 - A_1 x - \frac{A_1}{2} y & -\frac{A_1}{2} x \\ -\frac{A_2}{2} y & A_2 - A_2 y - \frac{A_2}{2} x \end{bmatrix}. \quad (2-4-2)$$

Evaluating Eq. (2-4-2) at the origin gives

$$J\underline{F} = \begin{bmatrix} A_1 & 0 \\ 0 & A_2 \end{bmatrix}. \quad (2-4-3)$$

Therefore, the origin is stable if both $|A_1| < 1$ and $|A_2| < 1$, and unstable if either $|A_1| > 1$ or $|A_2| > 1$.

Evaluating Eq. (2-4-2) at the fixed point given by Eq. (2-2-2b) gives

$$J\underline{F} = \begin{bmatrix} \frac{A_1}{A_2} & 0 \\ 1 - A_2 & 2 - A_2 \end{bmatrix}, \quad (2-4-4)$$

whose eigenvalues are $\lambda_1 = \frac{A_1}{A_2}$ and $\lambda_2 = 2 - A_2$. Therefore, the fixed point (2-2-2b) is stable if both $1 < A_2 < 3$ and $|A_1| < A_2$, and unstable if either $A_2 > 3$, $A_2 < 1$, or $|A_1| > A_2$.

Finally, evaluating Eq. (2-4-2) for the third fixed point, Eq. (2-2-2c) gives

$$J\underline{F} = \begin{bmatrix} 2 - A_1 & 1 - A_1 \\ 0 & \frac{A_2}{A_1} \end{bmatrix}. \quad (2-4-5)$$

This fixed point is stable if both $1 < A_1 < 3$ and $|A_2| < A_1$ and unstable if either $A_1 > 3$, $A_1 < 1$, or $|A_2| > A_1$.

The parameter values $A_1, A_2 = \{1, 3\}$ result in eigenvalues of magnitude one for Eqs. (2-4-4) and (2-4-5), and thus are boundaries of linear stability. Consider the case $A_2 = 3$ and A_1 arbitrary. The fixed point (2-2-2b) is unstable for $A_1 > 3$. For $A_1 \leq 3$, stability cannot be determined by linear analysis because at least one of the Jacobian matrix eigenvalues has unit magnitude. For $A_1 < 3$, numerical solutions have converged to this fixed point, indicating that it has a finite region of attraction. On the other hand, for $A_2 = 3$, the fixed point Eq. (2-2-2c) is stable if $1 < A_1 < 3$ and $|A_1| > 3$, which is a contradiction; so for $A_1 \neq 3$, this solution is unstable. This fixed point may be nonlinearly stable at $A_1 = 3$.

Consider further the degenerate case $A_1 = A_2 = A$. Evaluating Eq. (2-4-2) at the fixed point (2-2-2d) with $A_1 = A_2 = A$ yields

$$J\underline{F} = \begin{bmatrix} 1 - \frac{A[2 - \frac{2}{A} - y]}{2} & \frac{-Ay}{2} \\ -A \frac{[2 - \frac{2}{A} - y]}{2} & 1 - \frac{Ay}{2} \end{bmatrix}. \quad (2-4-6)$$

The eigenvalues of this matrix are $\lambda_1 = 1$ and $\lambda_2 = 2 - A$. Thus, the stability of this "off-axes" fixed point (fixed point with both species nonzero) is indeterminate. Figure 3 summarizes the results of the parametric stability analysis of the system (2-1-1).

2.5 DETERMINATION OF THE PARAMETRIC REGIONS WHICH YIELD STABLE PERIODIC SOLUTIONS

We showed in Section 2.3 that any periodic solution to Eqs. (2-1-1) for $A_1 \neq A_2$ must have at least one component zero. In this section, we determine the regions in parameter space, (A_1, A_2) , in which periodic solutions with either x or y zero may be stable. The Jacobian matrix for x or y zero simplifies significantly and its eigenvalues can be found analytically as follows. The Jacobian of the n th composition of the system is

$$J\underline{F}^n(x, y) = \begin{bmatrix} f_{1,x}^n & f_{1,y}^n \\ f_{2,x}^n & f_{2,y}^n \end{bmatrix} \quad (2-5-1)$$

where

$$\underline{F}^n(x, y) = \begin{bmatrix} f_1^n(x, y) \\ f_2^n(x, y) \end{bmatrix},$$

whose components are given by Eqs. (2-3-2).

Period- n solutions are essentially fixed points of the n th composition of the map and thus satisfy Eqs. (2-3-3). Consider, for example, a period- n solution of the form $[0, y]$. For this case, Eqs (2-3-1) become

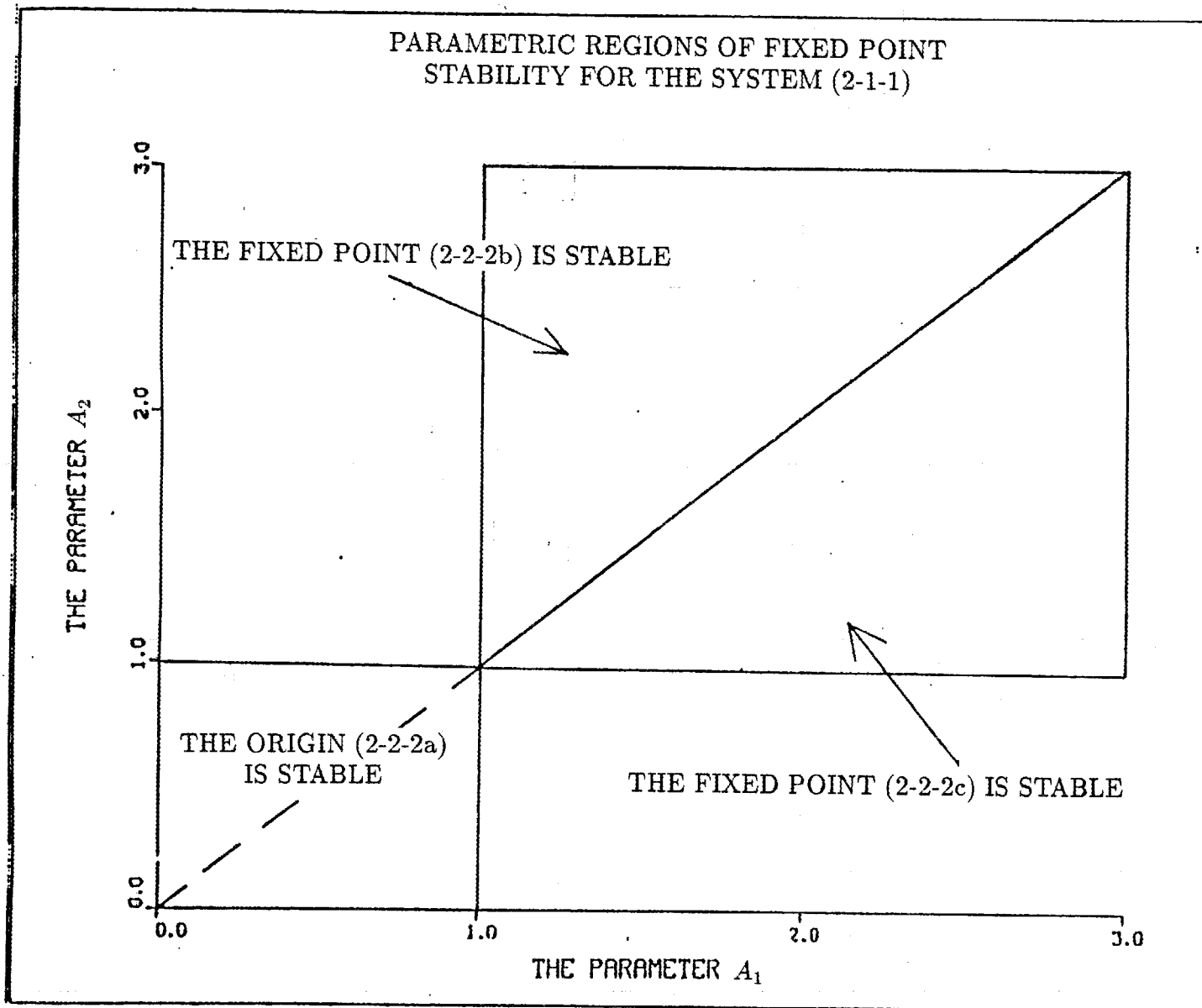


Figure 3. Stability diagram for the system (2-1-1).

$$\begin{aligned} f_1(0, y) &= 0 \\ f_2(0, y) &= A_2 y - \frac{A_2}{2} y^2 \end{aligned} \quad (2-5-2)$$

and the Jacobian of the system becomes

$$J\underline{F}(0, y) = \begin{bmatrix} A_1(1 - \frac{y}{2}) & 0 \\ -A_2 \frac{y}{2} & A_2(1 - y) \end{bmatrix} . \quad (2-5-3)$$

The Eqs. (2-3-3) become the single condition on the amplitude, y , of the period- n solution,

$$\frac{1}{A_2^n} = \left(1 - \frac{y}{2}\right) \prod_{i=1}^{n-1} \left(1 - \frac{f_2^i(0, y)}{2}\right) , \quad n > 1 . \quad (2-5-4)$$

The elements of the Jacobian, Eq. (2-5-1) can now be evaluated. Observe immediately $f_{1,y}^n(0, y)$ vanishes because $f_{1,y}(0, y)$ and $f_1(0, y)$ are zero. So, the eigenvalues are $f_{1,x}^n(0, y)$ and $f_{1,y}^n(0, y)$. Using Eqs. (2-5-2)–(2-5-4), these are now evaluated for $n > 1$.

First note $f_1^i(0, y) = 0$ because $f_1(0, y) = 0$ and f_1^i is given by Eq. (2-5-3). Then, by virtue of Eq. (2-5-4)

$$f_{1,x}^n(0, y) = A_1^n \left(1 - \frac{y}{2}\right) \prod_{i=1}^{n-1} \left(1 - \frac{f_2^i}{2}\right) = \frac{A_1^n}{A_2^n} . \quad (2-5-5)$$

Since $f_{1,y}^i(0, y) = 0$,

$$\begin{aligned} f_{2,y}^n(0, y) &= A_2^n \left(1 - \frac{y}{2}\right) \prod_{i=1}^{n-1} \left(1 - \frac{f_2^i}{2}\right) - A_2^n \frac{y}{2} \prod_{i=1}^{n-1} \left(1 - \frac{f_2^i}{2}\right) \\ &\quad + A_2^n y \left(1 - \frac{y}{2}\right) \sum_{i=1}^{n-1} \left(-\frac{f_{2,y}^i}{2}\right) \prod_{\substack{j=1 \\ j \neq i}}^{n-1} \left(1 - \frac{f_2^j}{2}\right) \end{aligned}$$

with all functions and derivatives evaluated at $[0, y]$.

Using Eq. (2-5-4),

$$\begin{aligned} f_{2,y}^n(0, y) &= 1 - A_2^n \frac{y}{2} \prod_{i=1}^{n-1} \left(1 - \frac{f_2^i}{2}\right) \\ &\quad + A_2^n y \left(1 - \frac{y}{2}\right) \sum_{i=1}^{n-1} \left(-\frac{f_{2,y}^i}{2}\right) \left(1 - \frac{f_2^i}{2}\right)^{-1} \left(\frac{1}{A_2^n (1 - \frac{y}{2})}\right) . \end{aligned}$$

Simplifying and writing the terms inside the summation as the derivative of the natural logarithm gives

$$f_{2,y}^n(0, y) = 1 - \frac{y}{2} \left(1 - \frac{y}{2}\right)^{-1} + y \sum_{i=1}^{n-1} \frac{\partial}{\partial y} \ln \left[1 - \frac{f_2^i}{2}\right] ,$$

or,

$$f_{2,y}^n(0, y) = 1 - \frac{y}{2} \left(1 - \frac{y}{2}\right)^{-1} + y \frac{\partial}{\partial y} \ln \left[\prod_{i=1}^{n-1} \left(1 - \frac{f_2^i}{2}\right) \right] .$$

Using Eq. (2-5-4) and then differentiating and simplifying gives

$$f_{2,y}^n(0, y) = 1 . \quad (2-5-6)$$

This immediately implies that the stability of the solution cannot be determined by linear analysis. However, it is minimally necessary for stability that the following condition be met:

$$|A_1| \leq |A_2| . \quad (2-5-7)$$

Essentially, the same analysis for the solution of the form $[x, 0]$ to the n th composition of Eqs. (2-3-1) yields the eigenvalues

$$f_{2,y}^n(x, 0) = \frac{A_2^n}{A_1^n}$$

$$f_{2,x}^n(x, 0) = 1 .$$

Again, linear analysis is insufficient. However, it tells us a necessary condition for stability of this solution is

$$|A_2| \leq |A_1| . \quad (2-5-8)$$

So, it has been shown in this section that linear analysis is insufficient to determine the stability of period- n solutions of Eqs. (2-1-1) for $n > 1$, although necessary constraints on A_1 and A_2 were found.

2.6 ANOMALOUS NUMERICAL SOLUTIONS

This section is motivated by the existence of anomalous periodic orbits in the finite precision computer simulation of Eqs. (2-1-1) with $A_2 = 3$ and $A_1 \leq 3$. The computer results conflict with the MACSYMA results which show no such orbits exist for those parameter values. Specifically, for $A_1 < 3$, the y -component of the single precision (i.e., seven significant figures) computed iterate oscillates indefinitely with period two about the y -component of the fixed point, Eq. (2-2-2b), namely $\bar{x} = 0, \bar{y} = 4/3$. The x -component converges monotonically to zero (see Figure 4). The periodicity of the y -component appears to be stable; after 50000 iterations to

damp the transients, every second iterate is identical up to the seven significant figures for some initial conditions (see Table 1).

TABLE 1
The Anomalous Periodicity of the y -Iterate of Eqs.(2-1-1)
Single Precision. For $A_2 = 3$, $A_1 = 0.1$, $x_0 = y_0 = .6$

<u>Iteration Number</u>	<u>y-component</u>
50,001	1.329810
50,002	1.336837
50,003	1.329810
50,004	1.336837

Similar behavior is exhibited for $A_1 = A_2 = 3$. Here, both the x - and y -component oscillated with period two about their respective values of a fixed point given by Eq. (2-2-2d). For $x_0 = y_0 = .6$, the iterates begin converging to the fixed point $\bar{x} = \bar{y} = 2/3$, but eventually oscillate about it (see Table 2).

TABLE 2
The Anomalous Periodicity of the Iterates of Eqs. (2-1-1)
Single Precision. For $A_2 = 3$, $A_1 = 3$, $x_0 = y_0 = .6$

<u>Iteration Number</u>	<u>x-Iterate</u>	<u>y-Iterate</u>
50,001	0.6685271	0.6685271
50,002	0.6647958	0.6647958
50,003	0.6685271	0.6685271
50,004	0.6647958	0.6647958

An analysis based on the computer's finite truncation, i.e., the number of significant figures the computer retains, was formulated to explain this contradiction between analytical and numerical results. A double precision program has been written, and it displays dynamical behavior consistent with that predicted by the truncation analysis. The truncation analysis is presented first, followed by an interpretation of the double precision results. The analysis is written with A_2 and A_1 arbitrary; however, so far, the only cases discussed are $A_2 = 3$ and $A_1 = A_2 = 3$.

Case 1: $x \neq 0, y \neq 0$

The family of fixed points is given by Eq. (2-2-2d). Suppose the average of x and y differs from the value $(1 - \frac{1}{A})$ by some real number δ_n after n iterations,

$$\frac{x_n + y_n}{2} - \left(1 - \frac{1}{A}\right) = \delta_n \quad (2-6-1)$$

Substituting Eq. (2-6-1) into Eqs. (2-1-1) yields

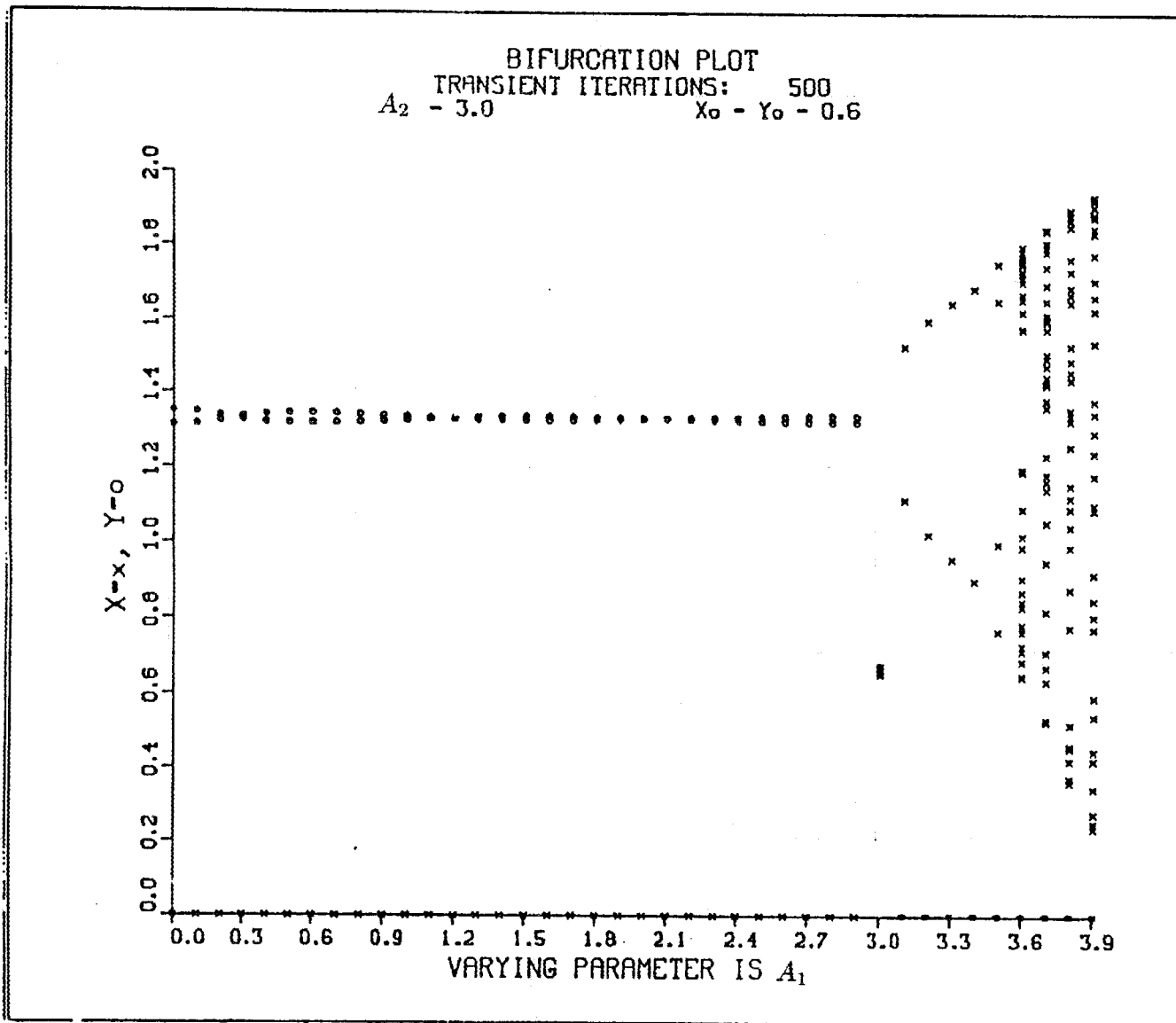


Figure 4. An example of the anomolous periodic solutions. The oscillations in species y are easily seen.

$$\begin{aligned}x_{n+1} &= x_n(1 - A\delta_n) \\y_{n+1} &= y_n(1 - A\delta_n) .\end{aligned}$$

The above can be rewritten as

$$\frac{x_{n+1} + y_{n+1}}{2} = \left(\frac{x_n + y_n}{2} \right) (1 - A\delta_n) .$$

Subtracting $(1-1/A)$ from both sides and using Eq. (2-6-1) yields,

$$\frac{x_{n+1} + y_{n+1}}{2} - \left(1 - \frac{1}{A} \right) = \delta_n(2 - A) - A\delta_n^2 \quad (2-6-2)$$

then applying Eq. (2-6-1) evaluated at $(n + 1)$, this becomes,

$$\delta_{n+1} = \delta_n(2 - A) - A\delta_n^2 . \quad (2-6-3)$$

Thus, the difference of the new iterate from the “fixed point” is related to the difference of the previous iterate from that “fixed point” by Eq. (2-6-2), which is, actually, another logistic map.

Case 2: $x = 0, y \neq 0$

The fixed point is given by Eq. (2-2-2b). Suppose the n th iterate differs from \bar{y} by some real number δ_n . So,

$$y_n - 2 \left(1 - \frac{1}{A_2} \right) = \delta_n \quad (2-6-4)$$

where $A_2 = 3$. Substituting Eq. (2-6-4) into Eqs. (2-1-1) yields

$$y_{n+1} = 2 \left(1 - \frac{1}{A_2} \right) + \delta_n(2 - A_2) - \frac{A_2}{2} \delta_n^2 \quad (2-6-5)$$

or

$$\delta_{n+1} = \delta_n(2 - A_2) - \frac{A_2}{2} \delta_n^2 . \quad (2-6-6)$$

Case 3: $x \neq 0, y = 0$

Similar analysis shows

$$x_{n+1} = 2 \left(1 - \frac{1}{A_1} \right) + \delta_n(2 - A_1) - \frac{A_1}{2} \delta_n^2 \quad (2-6-7)$$

or

$$\delta_{n+1} = \delta_n(2 - A_1) - \frac{A_1}{2} \delta_n^2 . \quad (2-6-8)$$

The evolution of the iterates is described by Eq. (2-1-1) or equivalently by Eqs. (2-6-2), (2-6-5), and (2-6-7), for cases 1, 2, and 3, respectively. In these expressions as the fixed point is approached, $\delta_n \rightarrow 0$ and δ_n^2 eventually assumes

values that are much smaller than the remaining terms which are of order 1 and δ_n . In particular, in a computing environment with N significant figures, once δ_n reaches values of the order $10^{-N/2}$, the terms proportional to δ_n^2 do not contribute to the evolution. When this happens, Eqs. (2-6-3), (2-6-6), and (2-6-8), with $A = 3$, $A_2 = 3$, and $A_1 = 3$, respectively, become,

$$\delta_{n+1} = -\delta_n, \quad \delta_n = O(10^{-N/2}) \quad (2-6-9)$$

on the computer, thus indicating oscillation of the iterates about the fixed point with an amplitude of the order $10^{-N/2}$. These oscillations result directly from the finite truncation on the computer and cannot be predicted by the exact analysis methods employed in the previous sections. Furthermore, they are bound to occur in any finite computing environment, even though its amplitude can be significantly reduced by increasing the number of significant figures, N , e.g., by computing in double precision.

For single precision variables in VAX FORTRAN, only about seven digits are significant. As an example, consider Eqs. (2-6-5) and (2-6-6) for $A_2 = 3$ and $\delta_0 = 1 \times 10^{-3}$ ($x_0 = 0$, $y_0 = 4/3 + \delta_0$). Via Eq. (2-6-5), $y_1 = 1.332331$, truncated after the seventh figure. One iteration of (2-6-6) gives $\delta_1 = -1.0015 \times 10^{-3}$; thus, $\delta_1^2 = 1.00300255 \times 10^{-6}$, exactly. The computer truncates this value when δ_1^2 is combined via Eq. (2-6-5) to form y_2 , only the first two digits of δ_1^2 will contribute. This is because the term $2(1 - \frac{1}{A_2})$ is of order 1, making the sixth decimal place the last significant figure. So, instead of the exact value for δ_1^2 , the value 1.0×10^{-6} is used in Eq. (2-6-5), yielding $y_2 = 1.334333 = y_0$. Thus, a fictitious period-two orbit is observed in this case.

In VAX FORTRAN, 16 figures are significant when working in double precision. Thus, "periodicity" analogous to the single precision results should be seen when variations in δ_n^2 are of order 10^{-16} , which will be truncated by the computer when the Eqs. (2-6-2), (2-6-5), and (2-6-7) are evaluated. A deviation of $\delta_0 = 10^{-8}$ from the fixed points occurring during the evolution would produce such variations. This deviation was initially supplied to the double precision program in a region in parameter space where Eqs. (2-6-5) and (2-6-6) represent the stable fixed point. Table 3 compares the values of y_n predicted by the analysis above to those calculated by the computer.

TABLE 3

A Verification of the Significant Figure Argument for Eqs. (2-1-1)

Double Precision. For $A_2 = 3$, $A_1 = 2$, $x_0 = 0$, $y_0 = 4/3 + \delta_n$, $\delta_n = 1 \times 10^{-8}$

<u>Iteration</u>	<u>y, predicted</u>	<u>y, calculated</u>
0	1.333333343333333	1.333333343333333
1	1.333333323333333	1.333333323333333
2	1.333333343333333	1.333333343333333

The above truncation analysis can also be verified in two other ways. First, it predicts the existence of fictitious period-two orbits for $A_1 = 3$ and $A_2 < 3$

analogous to those found for $A_2 = 3$ and $A_1 < 3$. This was confirmed on both the single and double precision simulators. Second, it predicts the appearance of a fictitious fixed point for $A = 1$, $A_2 = 1$, or $A_1 = 1$ in cases 1, 2, and 3, respectively, because again, convergence would depend on the quadratic term alone. Consider Eqs. (2-6-7) and (2-6-8). For the single precision program with $A_1 = 1$, they predict $x_0 = 1 \times 10^{-8}$, $y_0 = 0$ will be a fixed point because variations in x_n would be of order 10^{-16} and thus lost when combined with x_n . This was verified.

Thus, our truncation analysis predicts well the aberrations that arise in the computer simulation of Eqs. (2-1-1).

3. ANALYSIS OF A GENERALIZED TWO-SPECIES SYSTEM

3.1 INTRODUCTION

System (1-1-4) is itself quite complex. So as an aid in analysis, we first consider this system with neither linear attrition nor sources. We also couple the parameters B_1 and B_2 with C_1 and C_2 through the new parameter A to get:

$$\begin{aligned}x_{n+1} &= A_1 x_n (1 - (1 - A)x_n - A y_n) \\y_{n+1} &= A_2 y_n (1 - (1 - A)y_n - A x_n) .\end{aligned}\tag{3-1-1}$$

The fixed points of system (3-2-1) are determined analytically using MACSYMA and the results are presented in Section 3.2. Section 3.3 discusses the stability of the fixed points in parameter space. Section 3.4 describes the behavior of the map for a range of values of A . In particular, it discusses the instability that arises in system (3-1-1) for values of A approaching one, corresponding to low self-repression relative to bilinear attrition. A partially analytical basis for this pathological behavior is developed in Section 3.5. From the above analyses, conclusions are drawn in Section 3.6 to direct the subsequent numerical investigation of system (1-1-4) presented in Section 4.

3.2 DETERMINATION OF THE FIXED POINTS

Equations (3-1-1) are clearly a generalization of Eqs. (2-1-1) whereby the latter is obtained by setting

$$A = \frac{1}{2},\tag{3-2-1}$$

in the former.

The system (3-1-1) possesses four fixed points. The origin

$$\bar{x} = 0, \bar{y} = 0\tag{3-2-2a}$$

is a trivial fixed point. The fixed point

$$\bar{x} = 0, \bar{y} = -\frac{A_2 - 1}{(A - 1)A_2}\tag{3-2-2b}$$

exists for $A_2 \neq 0$ and $A \neq 1$. Similarly, the fixed point

$$\bar{x} = -\frac{A_1 - 1}{(A - 1)A_1}, \bar{y} = 0\tag{3-2-2c}$$

exists for $A_1 \neq 0$ and $A \neq 1$. Finally, the fixed point

$$\bar{x} = \frac{((2A - 1)A_1 - A + 1)A_2 - AA_1}{(2A - 1)A_1 A_2}, \bar{y} = \frac{((2A_1)A_1 - A)A_2 + (1 - A)A_1}{(2A - 1)A_1 A_2}\tag{3-2-2d}$$

exists for $A_1, A_2 \neq 0$ and $A \neq 1/2$. All fixed points were also found by a MACSYMA program.

3.3 LINEAR STABILITY OF THE FIXED POINTS

We now look for constraints on the parameters A_1 , A_2 , and A sufficient to ensure linear stability for each fixed points (3-2-2). Because of the complexity of the parametric expressions, surface plots have been generated in parameter space so that stable regions can be found by visual inspection.

Writing system (3-1-1) in vector form

$$\underline{G}(x, y) = \begin{bmatrix} A_1x(1 - (1 - A)x - Ay) \\ A_2y(1 - (1 - A)y - Ax) \end{bmatrix} . \quad (3-3-1)$$

The Jacobian of system (3-3-1) is

$$J\underline{G} = \begin{bmatrix} A_1 - 2A_1(1 - A)x - A_1Ay & -A_1Ax \\ -A_2Ay & A_2 - 2A_2(1 - A)y - A_2Ax \end{bmatrix} . \quad (3-3-2)$$

Evaluating the Jacobian (3-3-2) at the fixed point Eq. (3-2-2a) gives

$$J\underline{G} = \begin{bmatrix} A_1 & 0 \\ 0 & A_2 \end{bmatrix} .$$

Thus, the origin is stable if both $|A_1| < 1$ and $|A_2| < 1$. Evaluating the Jacobian at the fixed point (3-2-2b) yields

$$J\underline{G} = \begin{bmatrix} A_1 - \frac{A_1A(A_2-1)}{A_2(1-A)} & 0 \\ -\frac{A(A_2-1)}{(1-A)} & 2 - A_1 \end{bmatrix}$$

Thus, linear stability is assured if both $|2 - A_1| < 1$ and $|A_1 - \frac{A_1A(A_2-1)}{(1-A)A_2}| < 1$. Analogously, at the fixed point (3-2-2c),

$$J\underline{G} = \begin{bmatrix} 2 - A_1 & -\frac{A(A_1-1)}{(1-A)} \\ 0 & A_2 - \frac{A_2A(A_1-1)}{A_1(1-A)} \end{bmatrix} .$$

This fixed point is linearly stable if both $|2 - A_1| < 1$ and $|A_2 - \frac{A_2A(A_1-1)}{A_1(1-A)}| < 1$. Determination of the eigenvalues of the Jacobian (3-3-2) evaluated at the fixed point (3-2-2d) is exceedingly arduous. Therefore, a MACSYMA program was written and used to perform the evaluation.

Surfaces were generated in parameter space to give a graphical representation of the parametric regions of fixed-point linear stability. This was accomplished by using the graphics capabilities of MACSYMA and the DISPLA⁹ graphics

subroutine library. The surfaces generated for the "off-axes" (neither species zero) fixed point (3-2-2d) are shown in Figures 5 and 6.

3.4 NUMERICAL ANALYSIS OF THE BEHAVIOR OF SYSTEM (3-1-1) FOR VARIOUS VALUES OF THE PARAMETER A

If the self-repression terms are taken sufficiently large, system (3-1-1) displays interesting regimes, often with both species positive (see Figures 7, 8, 9, and 10). Stalemates, as well as clear victories, commonly occur, often in the same bifurcation diagram (see Figure 7). Periodicity and chaos are ubiquitous. Periodicity of a large number of cycles and chaos can be viewed as a loss of predictability in future force levels.

In the figures above, the effects of self-repression were over twice those of attrition. In a model of combat, we assume that the attrition effects should be generally taken significantly greater than the self-repression effects.

Therefore, we are particularly interested in parameter regions for which the self-repression is low. This implies the parameter A should be taken relatively close to one. Unfortunately, instability arises in the model (3-1-1) with increasing A . Here, instability means failure of the iterates to be attracted to any fixed, periodic, or chaotic attractor, resulting in the iterates of the species becoming unbounded. This behavior is consistent with the results of the last section which showed that as A approaches one, the fixed points (3-2-2b), (3-2-2c), and (3-2-2d) become repellers.

A series of bifurcation diagrams were plotted with A_2 first set to 3.55 and A_1 allowed to vary from zero to four. Bifurcation diagrams were constructed with $A = 0.3$ through $A = 0.9$ in 0.1 increments (see Figures 11, 12, 13, and 14).

As A becomes sufficiently large, instability arises, with iterates becoming unbounded for sufficiently large A_1 and then for even smaller A_1 as A grows larger.

The experiment was repeated with $A_2 = 1.7$. For a given A , decreasing A_2 has the effect of delaying the onset of instability until larger values of A_1 are reached. But for A greater than about 0.7, instability again arises, with iterates failing to converge to an attractor and becoming unbounded. With increasing A , the onset of this instability occurs for smaller values of A_1 .

In both cases ($A_2 = 3.55$ and $A_2 = 1.7$), for sufficiently small A_1 , the iterates of species x converge to zero, either monotonically or with decaying oscillations about zero (see Figure 15). The iterates of species y converge to a fixed, periodic, or chaotic attractor, depending on the values of A_1 and A_2 chosen. Iterates that decay monotonically can be forced into decaying oscillations by increasing either A_1 , A_2 , or A . Iterates which converge to zero with decaying oscillations can be forced to grow, again either by increasing A_1 , A_2 , or A sufficiently. These growing oscillations result in either species x or y becoming unbounded. Table 4 provides a sample of the numerical output showing how the amplitude of the oscillations increase with increasing A_1 for the same number of iterations.

3.5 THE EVOLUTION OF THE INSTABILITY

We now look at the transient behavior of the iterates for specific parameter regions to detail the evolution of the instability discussed above. First, consider the simplified case of zero self-repression in system (3-1-1), written

EIGENVALUE- -1 SURFACE OF THE OFF-AXES
FIXED POINT OF THE SYSTEM (3-1-1)

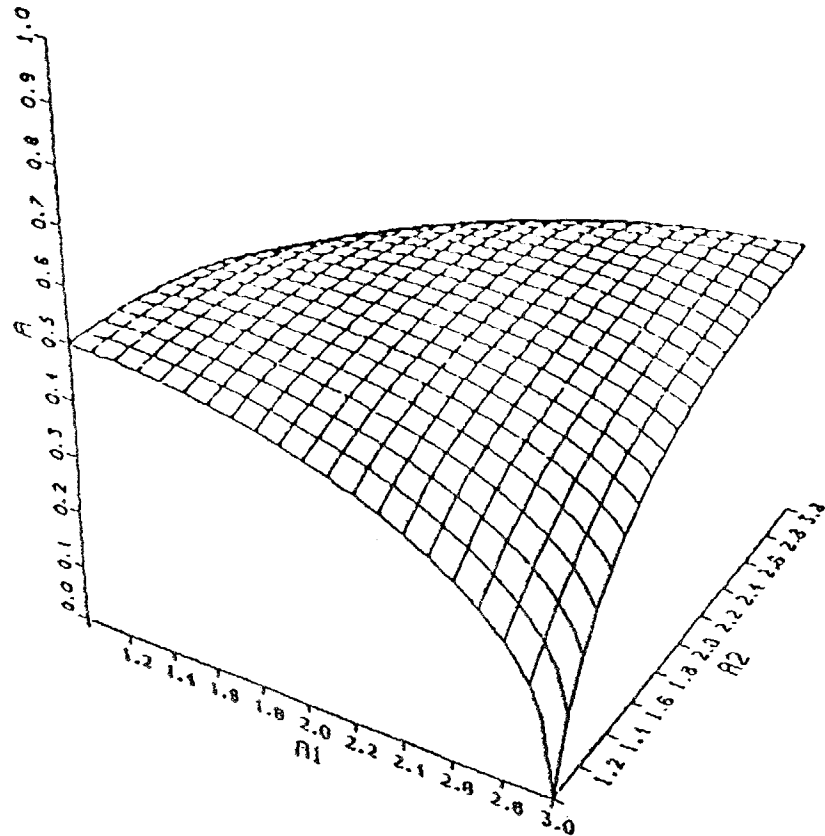


Figure 5. The region below this surface represents negative eigenvalues with magnitude less than one.

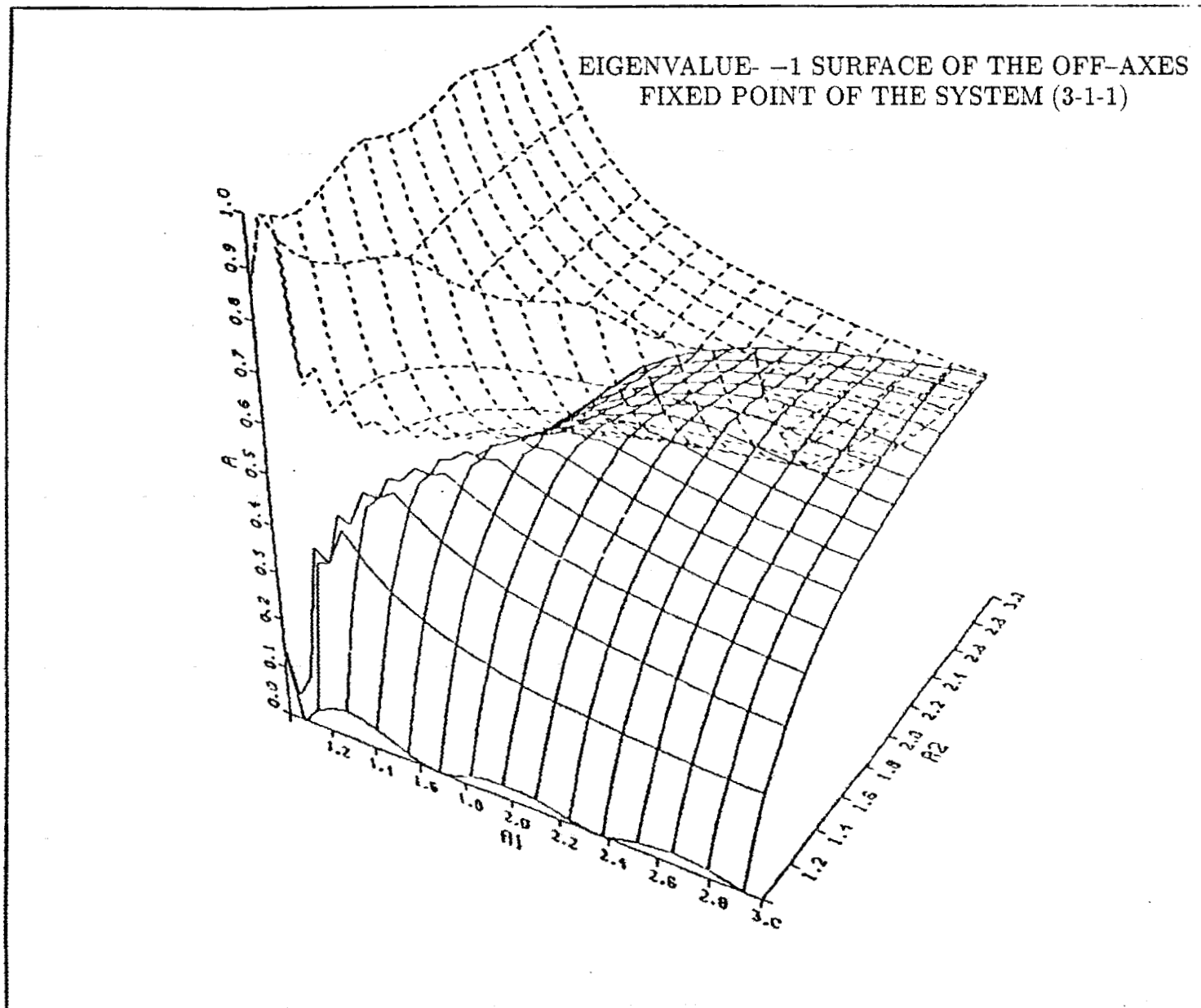


Figure 6. The region below the lower surface yields eigenvalues for the fixed point (3-2-2d) with magnitude less than one.

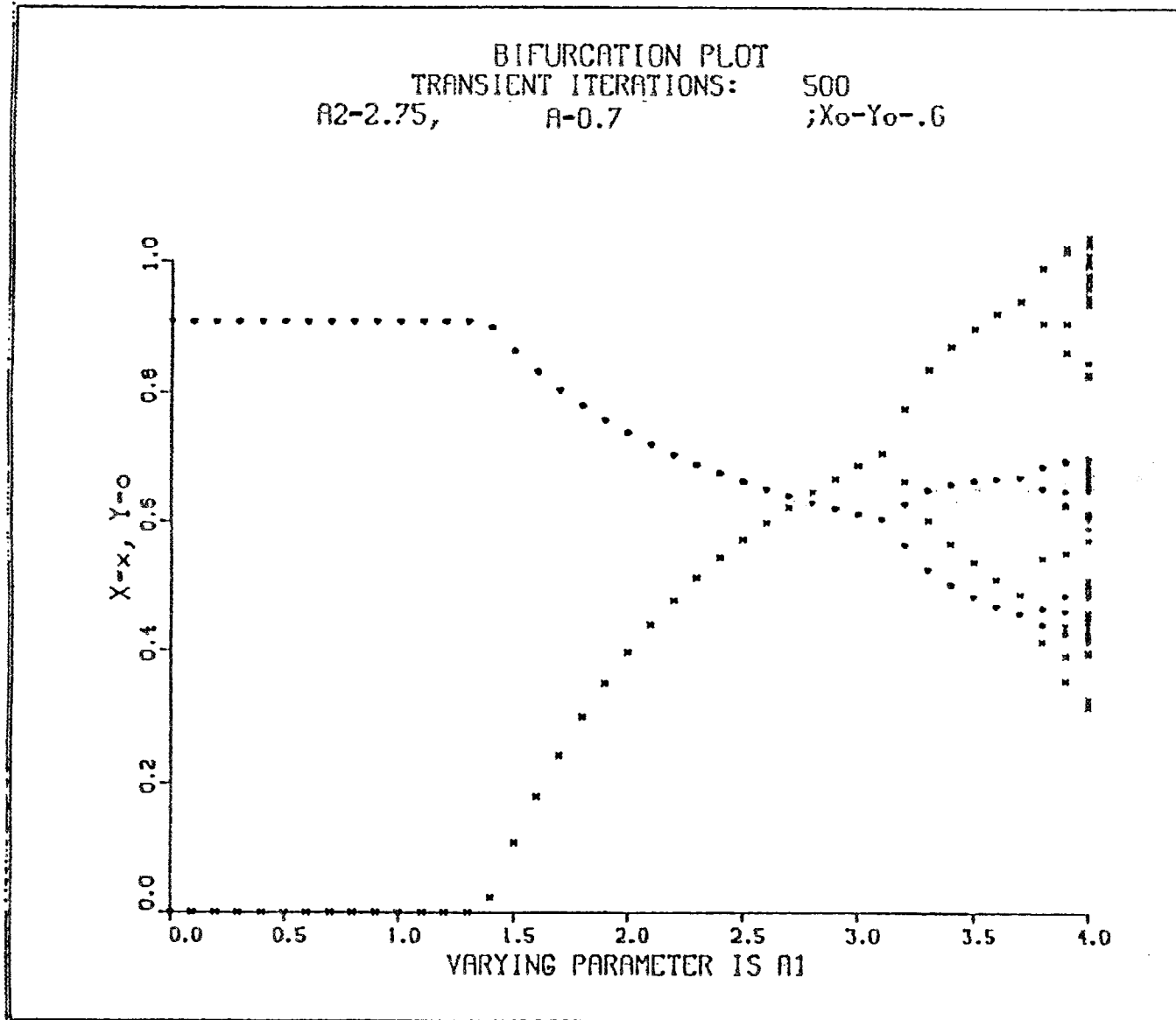


Figure 7. Bifurcation diagram for system (3-1-1).

BIFURCATION PLOT
 TRANSIENT ITERATIONS: 50000

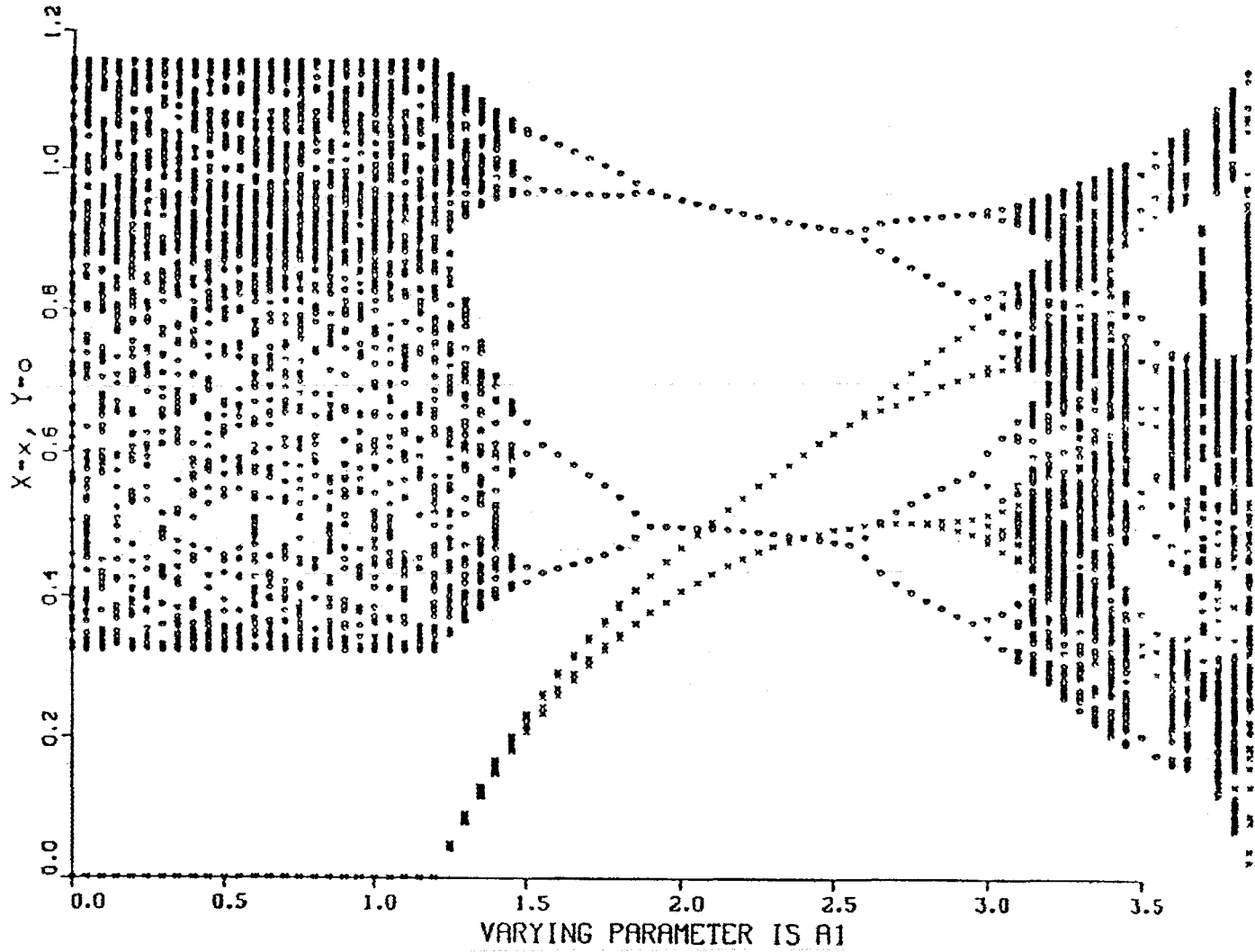


Figure 8. Bifurcation diagram for system (3-1-1) for $A_2 = 3.7$, $A = 0.2$, $x_0 = 0.5$, $y_0 = 0.6$.

BIFURCATION PLOT
TRANSIENT ITERATIONS: 50000

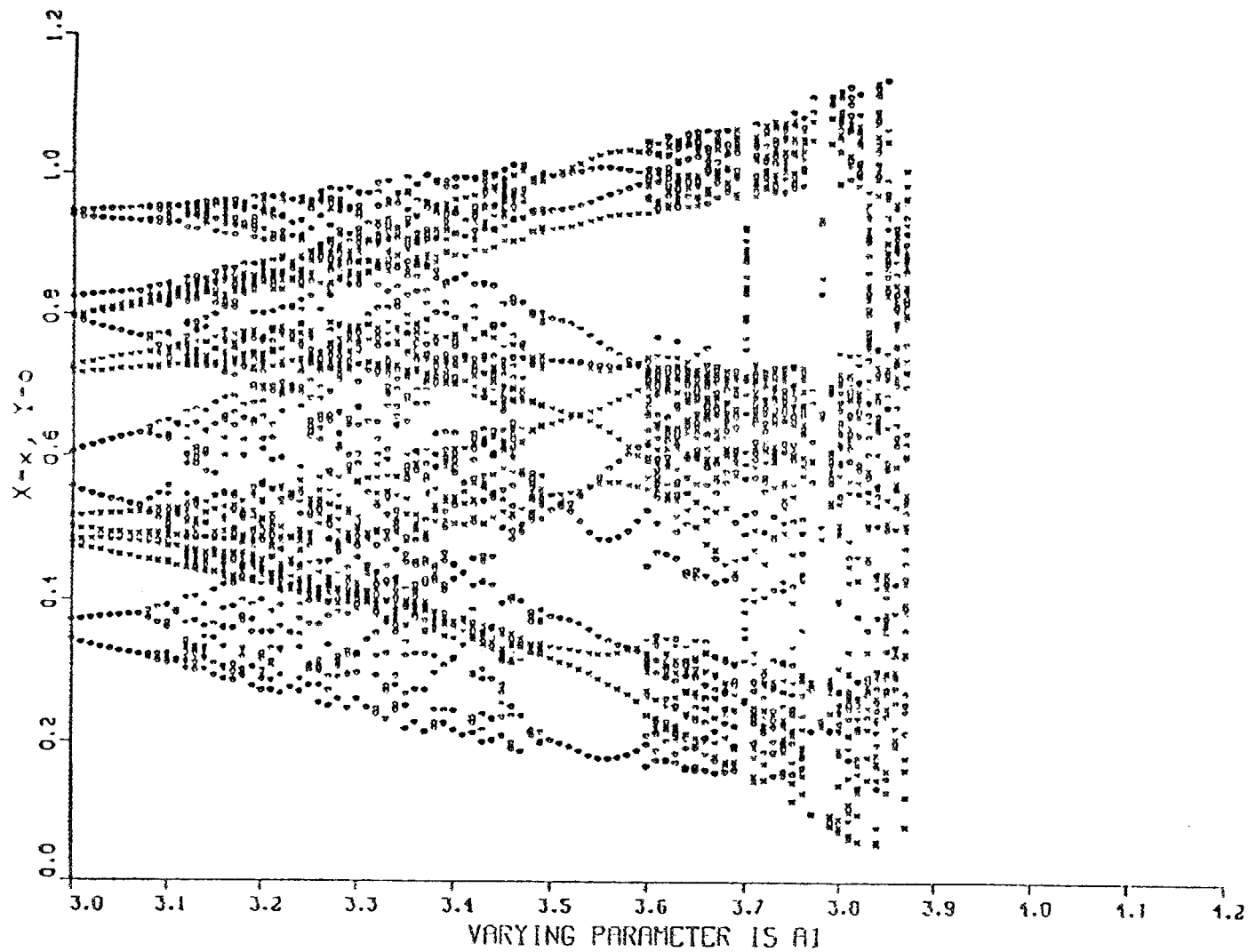


Figure 9. Bifurcation diagram for system (3-1-1) for $A_2 = 3.7$, $A = 0.2$, $x_0 = 0.6$, $y_0 = 0.5$.

Phase Portrait

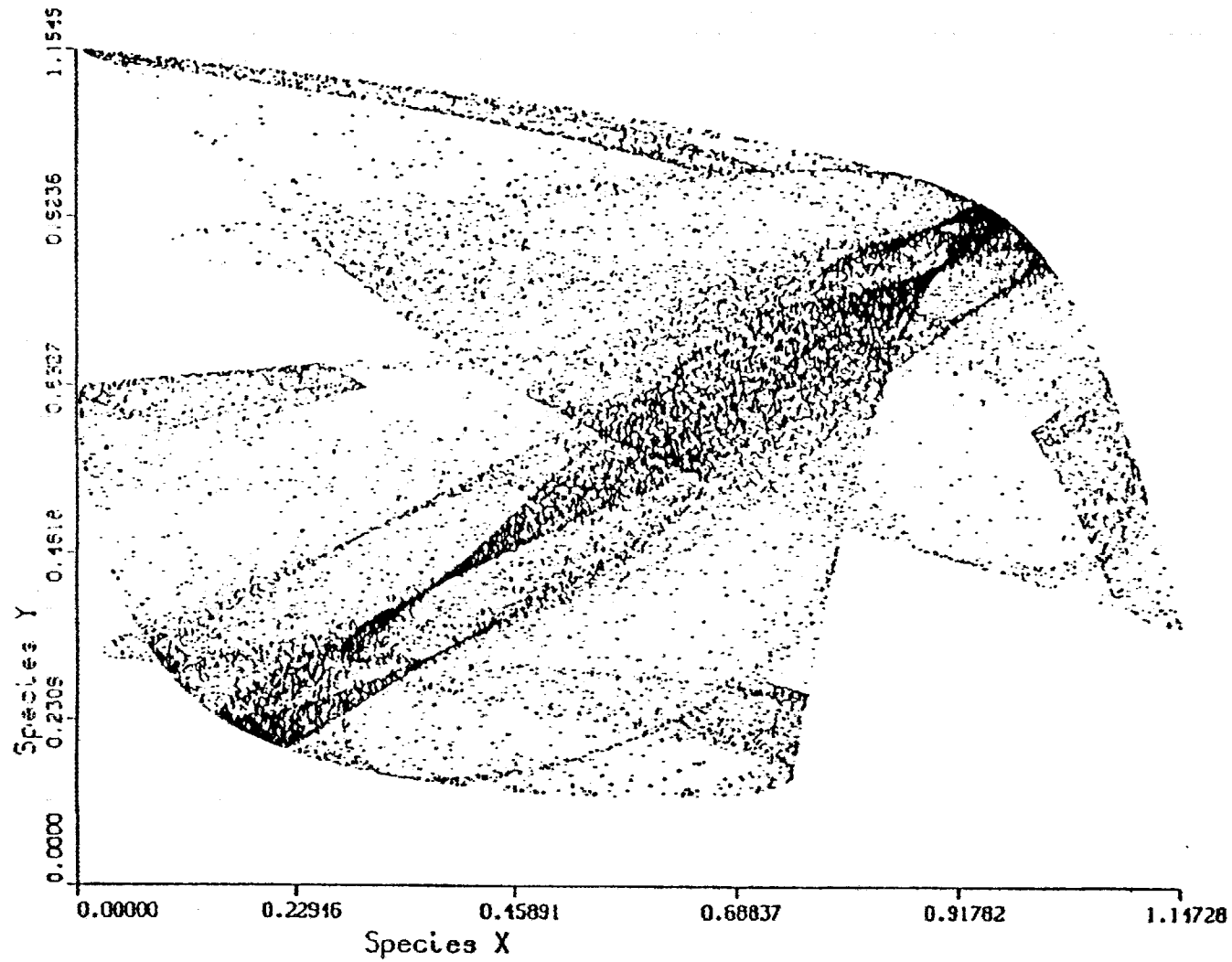


Figure 10. A chaotic attractor for system (3-1-1) for $A_1 = 3.87$, $A_2 = 3.7$, $A = 0.2$, $x_0 = 0.1$, $y_0 = 0.9$.

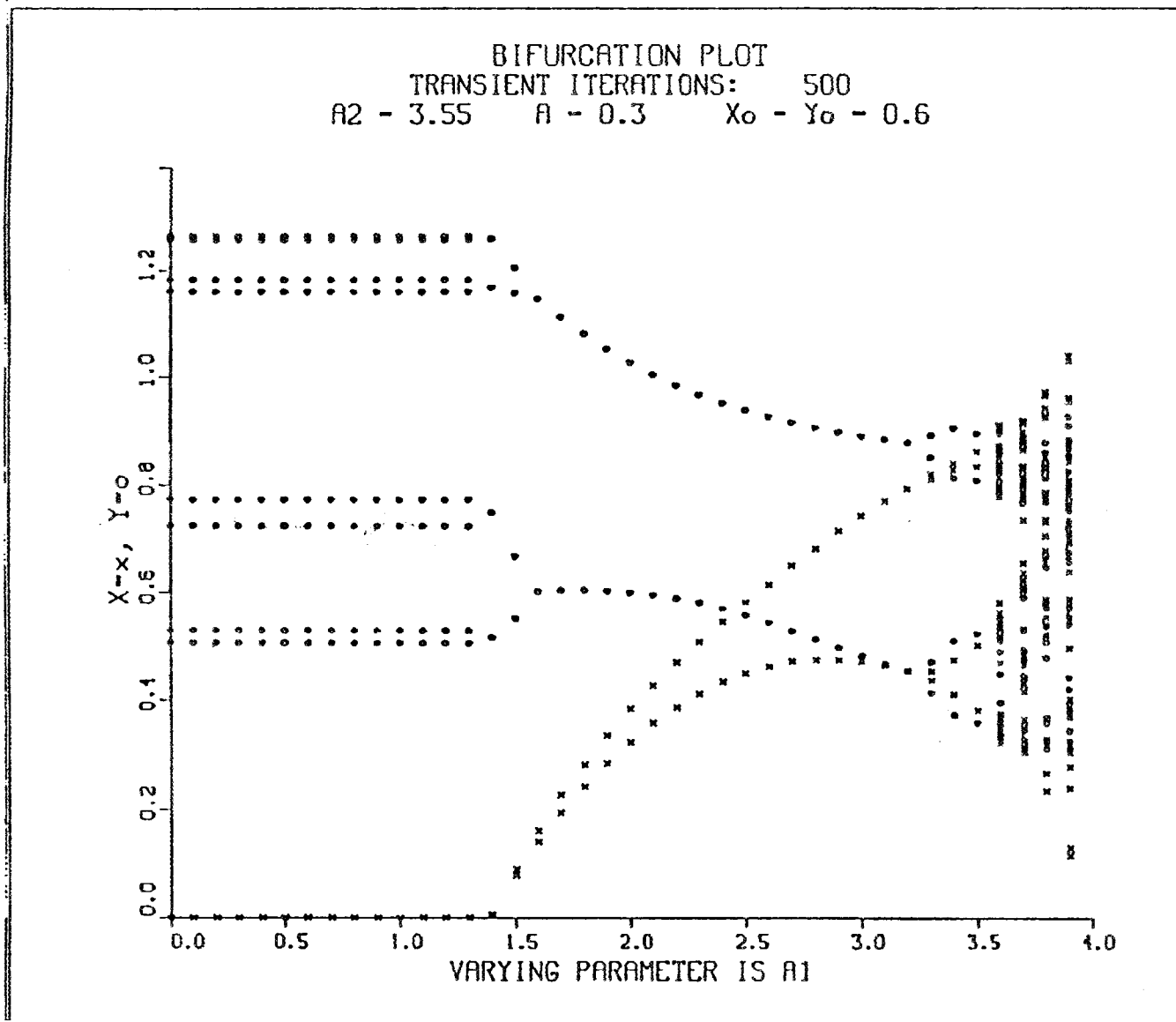


Figure 11. Bifurcation diagram for system (3-1-1).

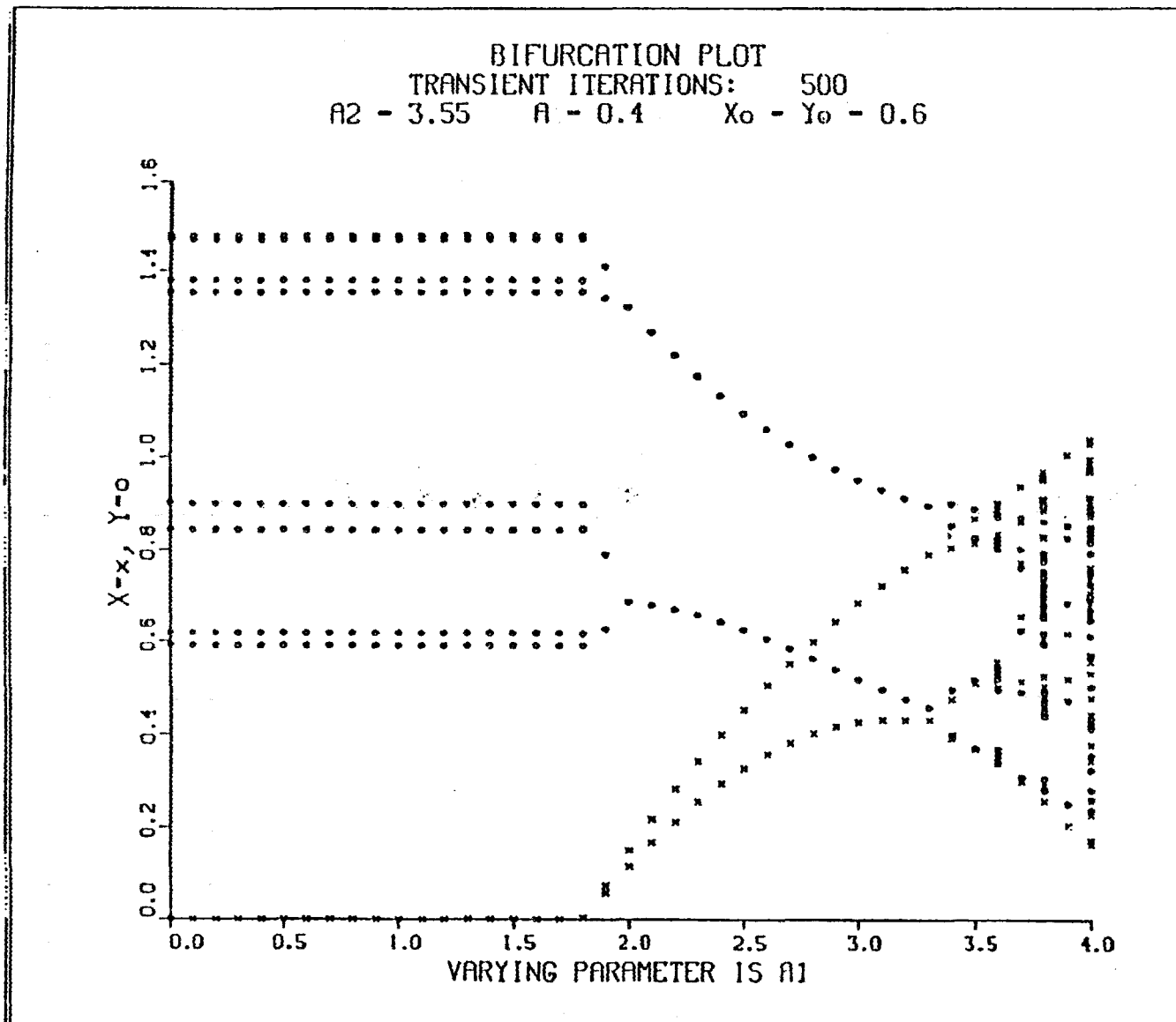


Figure 12. Bifurcation diagram for system (3-1-1).

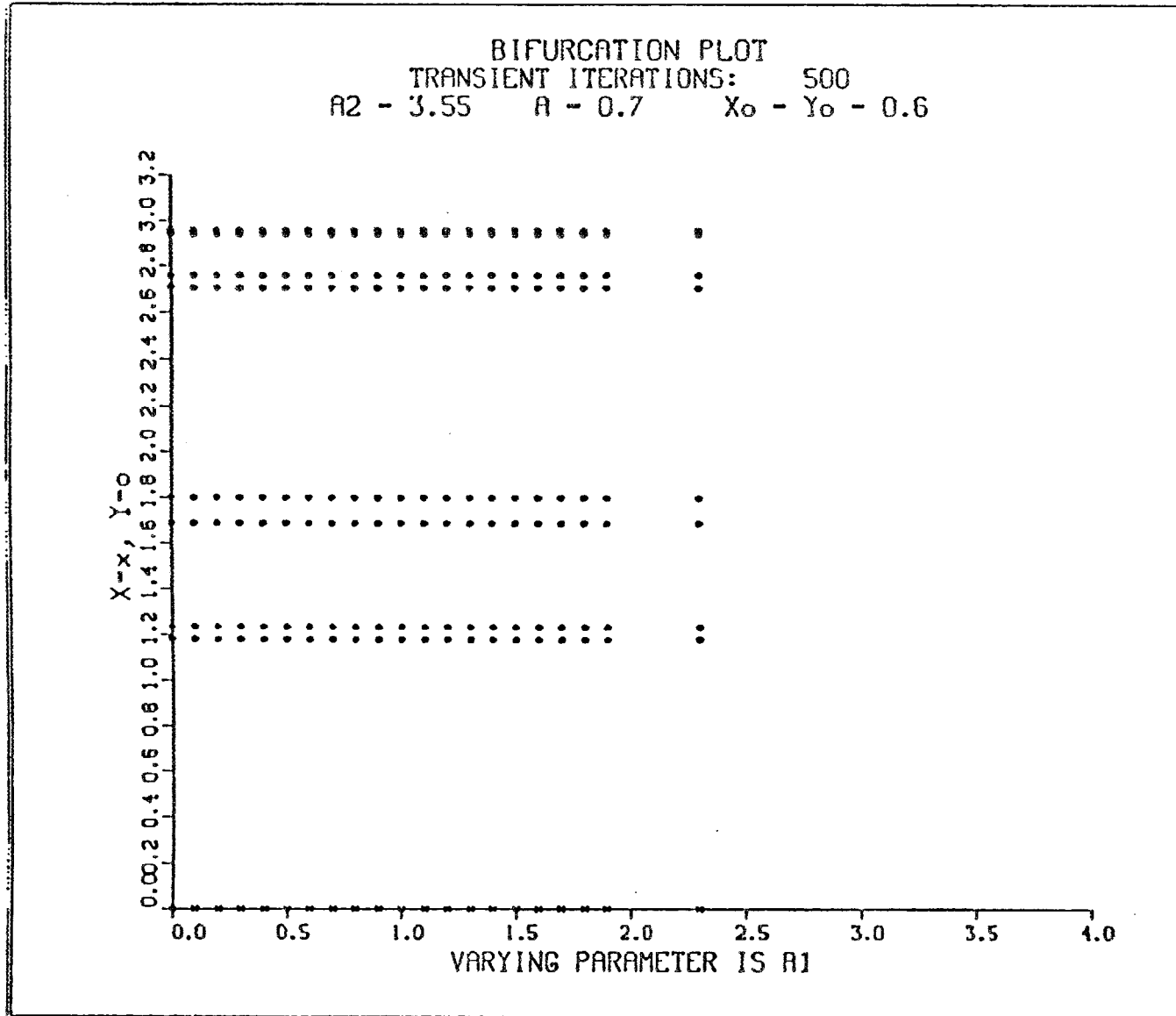


Figure 13. Bifurcation diagram for system (3-1-1). Iterates which became negative or unbounded were not plotted.

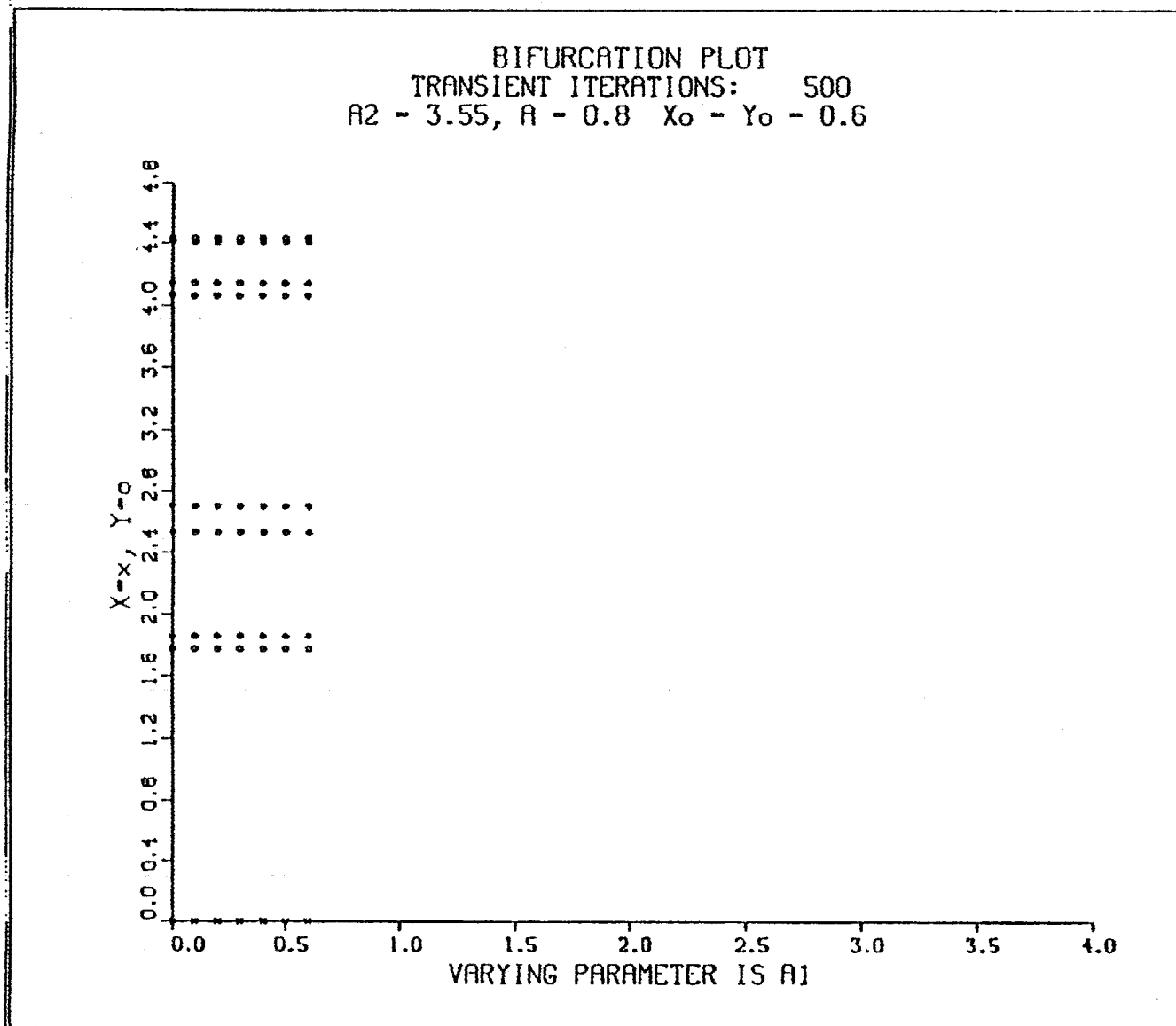


Figure 14. Bifurcation diagram for system (3-1-1). Iterates which became negative or unbounded were not plotted.

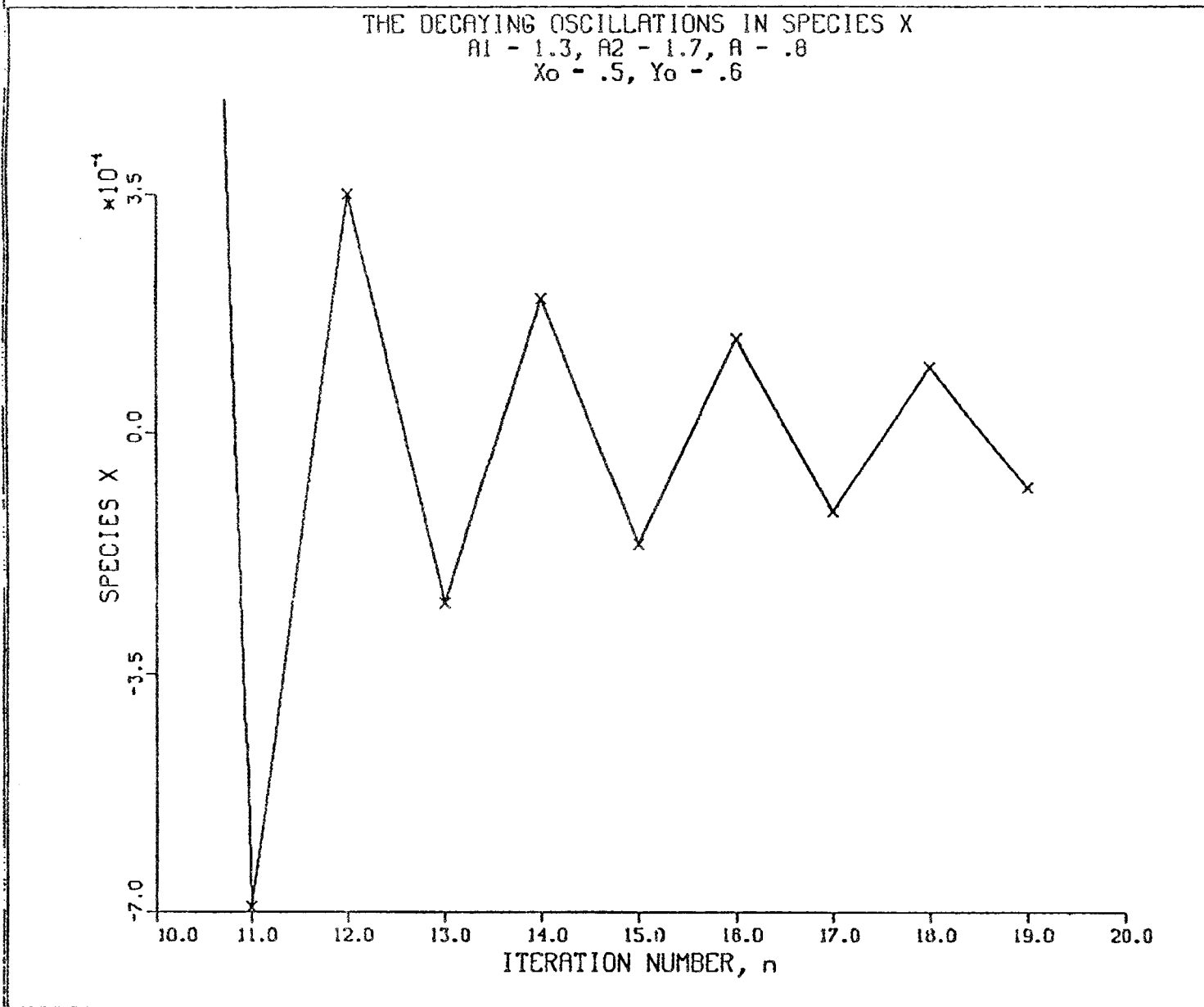


Figure 15. Decaying oscillations of species x.

TABLE 4

The increasing magnitude of the oscillations in species x for increasing A_1 in system (3-1-1) with $A = 0.7$, $x_0 = y_0 = 0.6$, $A_2 = 3.55$. These transients eventually reach a steady-state at zero.

Iteration	$A_1 = 1.1$	$A_1 = 1.6$	$A_1 = 2.3$
101	-5.545×10^{-33}	-3.428×10^{-19}	4.020×10^{-6}
102	5.466×10^{-33}	5.800×10^{-19}	1.590×10^{-6}
103	-1.569×10^{-33}	1.261×10^{-19}	3.278×10^{-6}
104	1.825×10^{-33}	-1.880×10^{-19}	1.967×10^{-6}
105	2.730×10^{-34}	5.443×10^{-20}	-4.784×10^{-6}
106	-2.797×10^{-34}	-9.323×10^{-20}	-1.498×10^{-6}
107	5.564×10^{-35}	-2.567×10^{-20}	3.208×10^{-6}
108	-6.552×10^{-35}	-3.681×10^{-20}	-1.337×10^{-6}

$$\underline{F} = \begin{bmatrix} A_1 x(1 - Ay) \\ A_2 y(1 - Ax) \end{bmatrix} . \quad (3-5-1)$$

The fixed point of system (3-5-1) with both species nonzero is

$$\bar{x} = \frac{A_2 - 1}{A_2 A} , \quad \bar{y} = \frac{A_1 - 1}{A_1 A} . \quad (3-5-2)$$

Evaluating the Jacobian of Eqs. (3-5-1) at the fixed point (3-5-2) yields the eigenvalues

$$\lambda_{1,2} = 1 \pm \sqrt{(A_1 - 1)A_2 - A_1 + 1} .$$

This immediately implies the fixed point (3-5-2) is linearly unstable for all parameter values, except $A_1 = A_2 = 1$. However, this caveat can be ignored in a modeling context because taking A_1 or $A_2 = 1$ corresponds to the absence of resupply and will necessarily result in trivial or negative steady-state solutions in at least one species. Therefore, in this idealized case of zero self-repression, a steady-state, non-oscillatory solution with both species nonzero cannot exist. In fact, it can be easily shown that all fixed points of the system (3-5-1) are linearly unstable for $A_1, A_2 \geq 1$.

With this in mind, consider Column A of Table 5 which shows successive iterates of system (3-5-1) for the parameter values listed. Notice that species y grows stronger while species x tends toward zero at first. However, after sufficient iterations, species x becomes negative and begins to oscillate about zero with increasing amplitude. This occurs because species y increases past one, so that

TABLE 5

The evolution of the instability in System (3-1-1) for various parameter values. The base 10 exponential is written using computer "E" notation.

Parameter Values	Column							
	A		B		C		D	
	$A_1 = 1.3 \ A_2 = 1.7$ $A = 0.8$ (System 3-2-5)		$A_1 = 1.3 \ A_2 = 1.7$ $A = 0.8$ (System 3-2-1)		$A_1 = 1.3 \ A_2 = 2.7$ $A = 0.8$ (System 3-2-1)		$A_1 = 1.3 \ A_2 = 1.7$ $B_1 = B_2 = 0 \ C_1 = C_2 = 0.8$ $D_1 = 0 \ D_2 = 0.4$ (System (1-1-4))	
Initial Conditions	$x_0 = 0.5$	$y_0 = 0.6$	$x_0 = 0.5$	$y_0 = 0.6$	$x_0 = 0.5$	$y_0 = 0.6$	$x_0 = 0.5$	$y_0 = 0.6$
Species Iteration	x	y	x	y	x	y	x	y
1	0.338	0.612	0.273	0.489	0.273	0.777	0.338	0.412
2	0.224	0.759	0.196	0.569	0.114	0.31	0.294	0.375
3	0.114	1.05	0.129	0.705	-1.11E-2	2.29	0.267	0.370
4	2.27E-2	1.63	6.88E-2	0.905	1.19E-2	3.40	0.244	0.387
5	-9.11E-3	2.70	2.33E-2	1.17	-2.69E-2	2.84	0.219	0.432
6	1.40E-2	4.67	1.65E-3	1.49	4.44E-2	3.47	0.186	0.432
7	-4.99E-2	7.85	-4.16E-4	1.77	-0.103	2.52	0.142	0.673
8	0.343	13.8	2.27E-4	1.94	0.134	3.93	8.55E-2	0.957
9	-4.51	17.1	-1.65E-4	2.02	-0.380	1.11	2.59E-2	1.48
10	74.4	134.1	1.32E-4	2.04	-9.21E-2	3.25	-6.28E-3	2.45
11	-10298	-13366	-1.09E-4	2.05	0.189	3.71	7.88E-3	4.20
12	—	—	9.19E-5	2.05	-0.495	1.053	-2.42E-2	7.09
13	—	—	—	—	-0.165	3.37	0.147	12.3
14	—	—	—	—	0.357	4.16	-1.69	18.3
15	—	—	—	—	-1.11	-1.34	30.1	74.3
16	—	—	—	—	-3.35	-7.88	-2293	-2936
17	—	—	—	—	-34.7	-112.0	—	—
					-4409	-15489	—	—

the attrition of species x surpasses its resupply, forcing x to become negative and to oscillate. The increasing magnitude of species y corresponds to the increasing amplitude of the oscillations of species x .

The final result is species x and y converging to minus infinity. However, we have not shown that this is the only type of behavior system (3-5-1) can exhibit. The iterates may instead remain bounded by converging to a periodic or possibly a chaotic attractor. However, for a variety of parameter values, unstable behavior was the only type observed.

Now consider the effect on the unstable behavior of system (3-5-1) of adding a small amount of self-repression; that is, we now consider system (3-1-1) for A large but less than one. Intuitively, self-repression might have the effect of curbing the drastic rise in species y . Certainly, this is the effect of the quadratic term in the single species logistic equation, for without it the iterates increase linearly without

bound. Observing Column B of Table 5, this seems to be the effect of quadratic self-repression in system (3-1-1) as well. The oscillations in species x now decay instead of grow. This would seem to be a result of the slower and bounded rise in species y .

Column C of Table 5 shows the effect of increasing the parameter A_2 on the dynamics above. Comparing Columns B and C, we see that the increase results in the return of the instability. As was mentioned in Section 3.4, increasing the parameter A_1 has a similar effect.

We hypothesized that the inclusion of a linear attrition term (aimed fire) to the y -equation of system (3-1-1) might help stunt the growth of the y -iterates, resulting in a stable system. The results are shown in Column D of Table 5. Obviously the attempt failed, probably because the effect of the linear attrition term becomes negligible as species x becomes close to zero, allowing the y -iterates to again rise.

3.6 CONCLUSIONS

In summary, the quadratic effect diminishes as A grows large. As even very small quadratic self-repression does not result in unboundedness in the absence of bilinear attrition, it is the combination of the lack of damping due to the low self-repression and the feedback of the bilinear terms that brings on instability.

We observed further increases in instability as A_1 and A_2 were increased.

The three general types of behavior observed for system (3-1-1) with large A are:

- (i) The iterates become unbounded. Generally, one species increases in strength, eventually forcing the other species into growing oscillations around zero, finally resulting in both iterates becoming unbounded.
- (ii) The iterates remain bounded with one iterate converging to zero monotonically and the other converging usually to a fixed attractor.
- (iii) The iterates remain bounded with one iterate converging to zero with decaying oscillations and the other converging to a fixed, periodic or chaotic attractor. For a given A , this behavior occurs for A_1 or A_2 larger than in (ii). The possibility of selecting parameters in such a way as to drive one species toward a fixed point while the other one is in a high bifurcation or even chaotic regime seemed a rather new phenomenon with promising potential for applications.

For many of the stable regions with low self-repression, one iterate converges to zero with decaying oscillations about zero. This means that positivity is not preserved in the iterates, which is physically unacceptable. However, the magnitudes of these transient oscillations are small, such that they could be taken to be zero.

Essentially, we have shown in the previous sections that for small quadratic effects in system (3-1-1), one species quickly gains a decisive advantage over the other, forcing the other to zero or into growing oscillations leading to unboundedness. This conclusion provides the rationale for the form of the numerical investigation of system (1-1-4) presented next.

4. NUMERICAL ANALYSIS OF SYSTEM (1-1-4)

4.1 INTRODUCTION

A brief description of the program used for the numerical simulations is presented in Section 4.2. In Section 4.3, we analyze system (1-1-4) without linear attrition. We consider system (1-1-4) with linear attrition in Section 4.4.

4.2 DESCRIPTION OF THE COMPUTER PROGRAM

A computer program called DPMAP,⁷ written in double-precision VAX FORTRAN,^{6,11} was used for the numerical analysis. It is based on an earlier program by S. de Rada called MAP.⁶ The form of the equations to be iterated is specified by the user in the subroutine DPEQN.FOR, which is contained in an external file. The user specifies parameter values and other options in the data file DPMAP.DAT. An output file with the numerical results is generated by the program, as well as a graphics file created using DISSPLA⁹ graphics subroutine library. The program is menu driven by a Digital Command Language¹² command file.

4.3 NUMERICAL ANALYSIS OF SYSTEM (1-1-4) FOR BILINEAR ATTRITION AND LOW SELF-REPRESSION

In an attempt to improve the stability of system (1-1-4) for low self-repression, we now decouple the parameters B_1 , B_2 , and C_1 , C_2 . We chose $B_1 < B_2$ and $C_1 < C_2$, effectively strengthening species x relative to the coupled-parameter case, system (3-1-1). Of course, this implies A_1 must be taken less than A_2 , otherwise, species x would necessarily emerge as dominant.

It was supposed that strengthening species x might help damp the increase in species y , allowing the iterates to remain bounded for a larger range of parameter values. It was also hoped that the strengthening of species x might allow the iterates to converge to an attractor positive everywhere, as commonly occurs in this system for larger quadratic effects. Besides being more interesting dynamically, this would mean system (1-1-4) with bilinear attrition would be capable of modeling stalemates for small quadratic effects.

The parameters A_1 , A_2 , B_1 , B_2 , C_1 , and C_2 were systematically varied and several bifurcation diagrams were constructed. The parameter A_2 was first chosen to be 2.75, a compromise between the need to reduce the strength of the species y and the desire to maintain the possibility for bifurcations into periodic orbits and chaos. The parameter A_1 was allowed to vary between zero and three. A reference case with $A_2 = 2.75$, $B_1 = B_2 = 0.3$, and $C_1 = C_2 = 0.7$ was constructed for comparison (see Figure 16).

Figures 17 and 18 show what we continued to see for all trials: a limited region of stability, always with one species converged to zero, which gives way to instability as A_1 is increased. The nature of this instability is the same as was found in system (3-1-1) and discussed in the previous two sections.

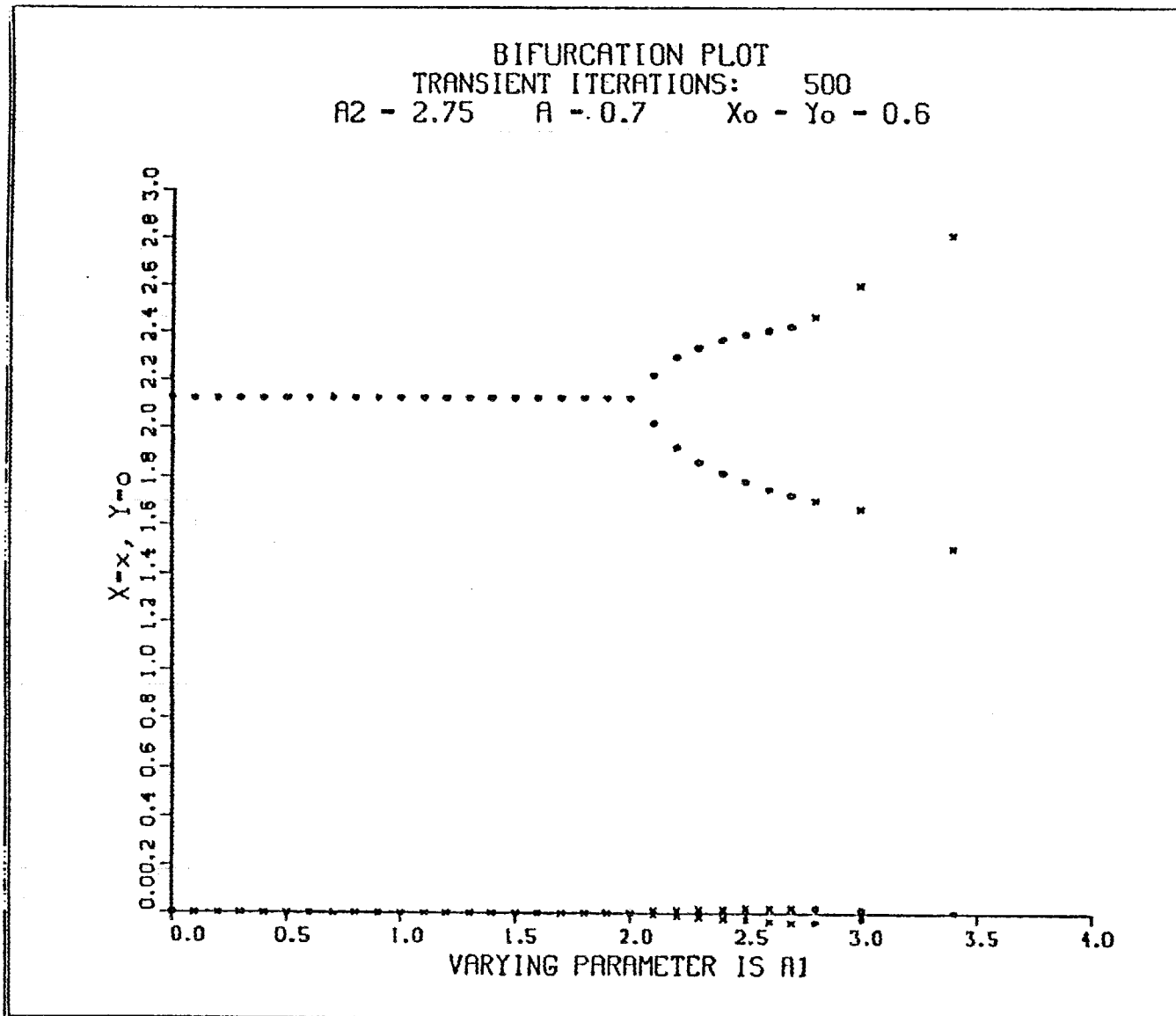


Figure 16. Reference case for a numerical analysis of system (1-1-4).

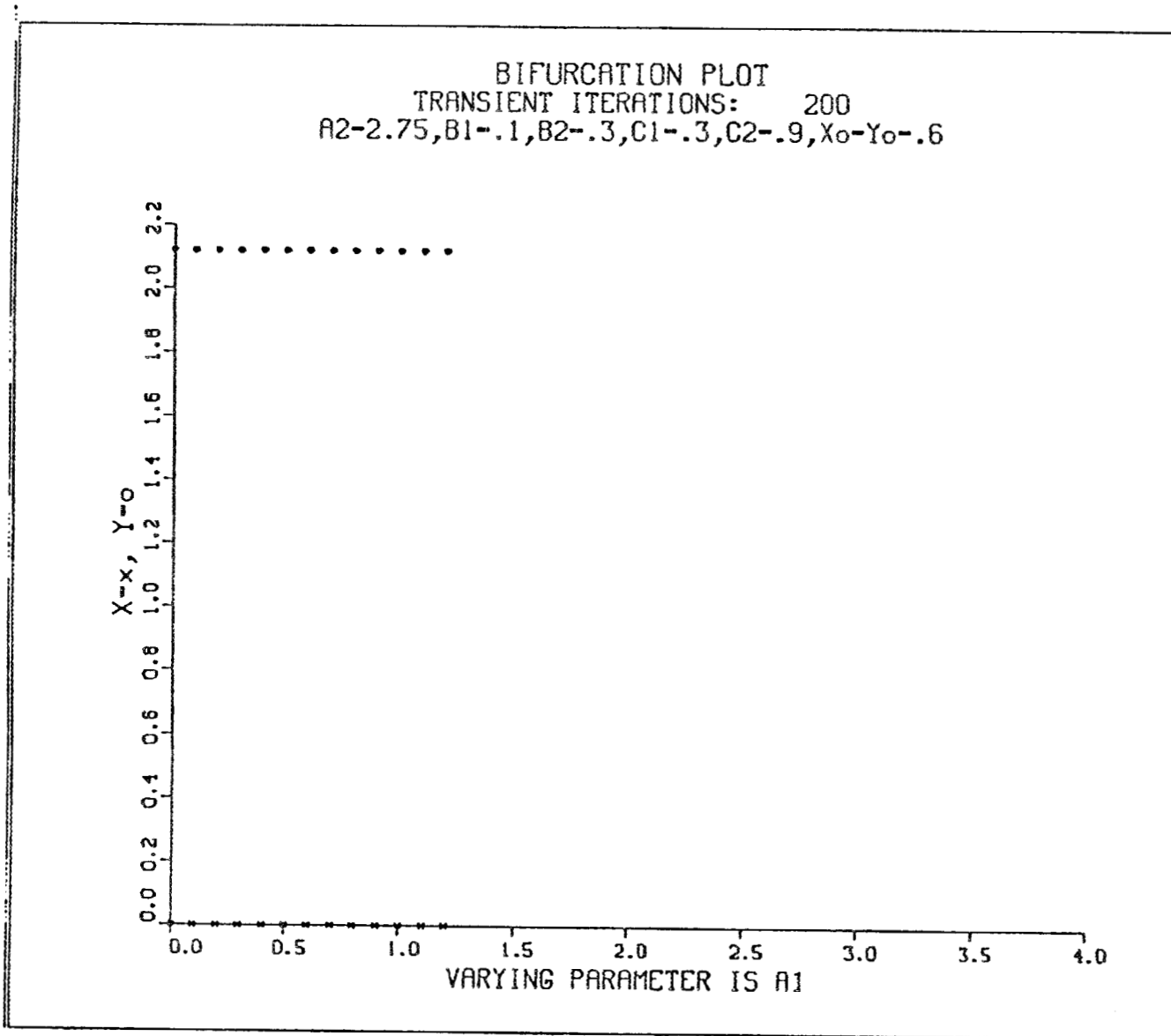


Figure 17. Bifurcation diagram for system (1-1-4). Iterates which became negative or unbounded were not plotted.

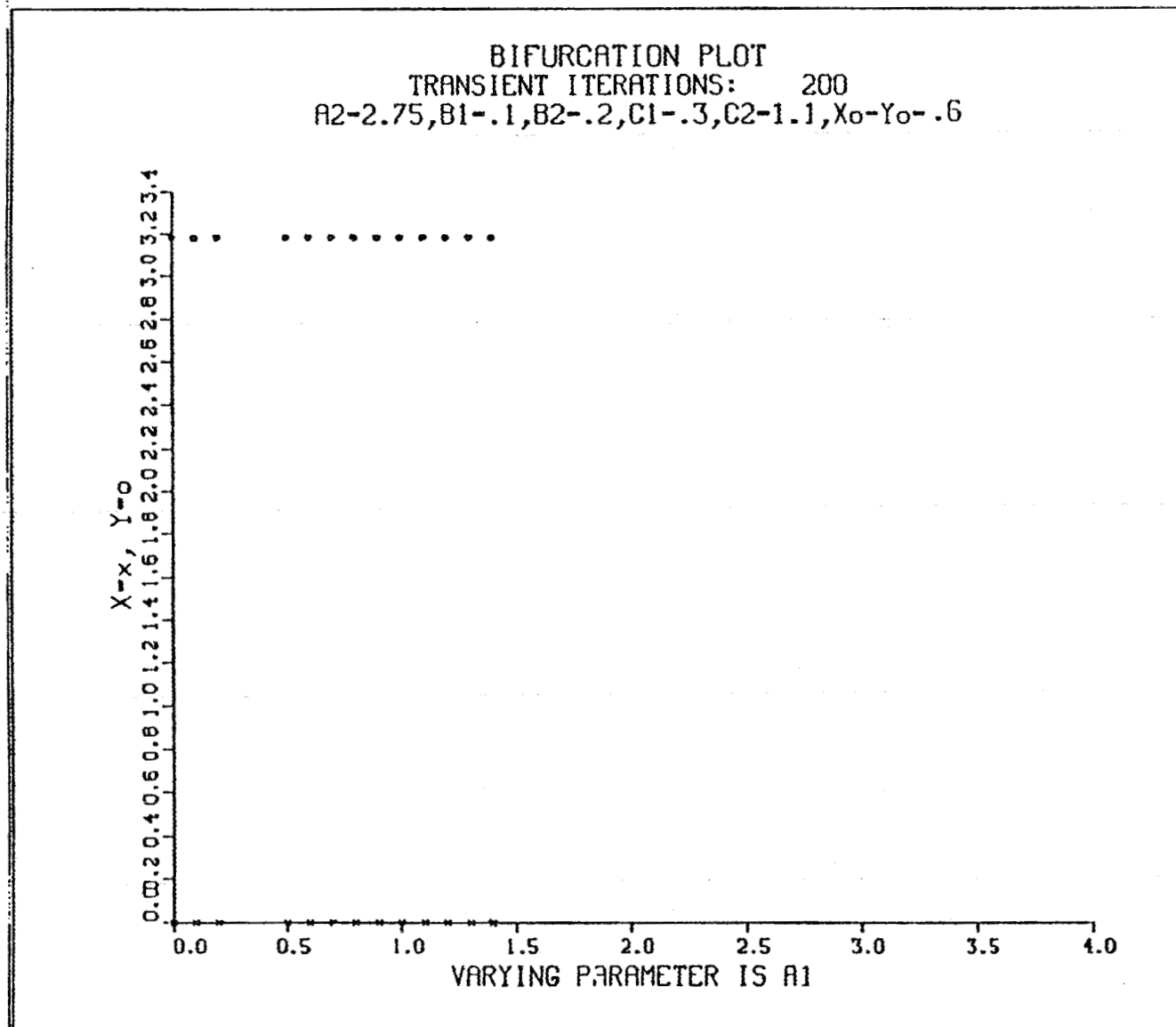


Figure 18. Bifurcation diagram for system (1-1-4). Iterates which became negative or unbounded were not plotted.

If a source term for species x is included, species x converges to the approximate value of the source term instead of zero. However, the inclusion of these terms in a model already containing resupply terms is questionable.

Of course, if the bilinear attrition of species y is increased beyond certain values, species x gains the advantage, even for A_1 less than A_2 . In trials where species x is made the stronger by increasing either the attrition of species y or the initial force-level of species x , the only stable behavior was, similar to the case before, the decay of species y to zero and the convergence of species x to a fixed, periodic, or chaotic attractor. However, there was an exception: stable periodic oscillations in both species. But from a modeling standpoint, this case must be ignored because some iterates would become negative and not of negligible magnitude.

We also analyzed the effect of granting both species equal strength (equal parameters) and equal initial force levels and then perturbing the values slightly. This was both an attempt to study the sensitivity of the dynamics to small parameter changes and an attempt to produce a steady-state solution with both species nonzero. We felt a steady-state solution with both species nonzero might occur if the strengths of the species were nearly equal. Table 6 shows the results of one such experiment. Obviously, the dynamics are highly sensitive to perturbations in the parameters and initial conditions from the symmetric case. Small perturbations in equal configurations of the forces were always seen to result in the annihilation of one species.

In summary, we have shown that system (1-1-4) with bilinear attrition and relatively small self-repression displays the same instability as system (3-1-1) and that decoupling of the parameters in system (1-1-4) has not helped to eliminate or even reduce the occurrence of the instability. The asymptotic states for low self-repression and bilinear attrition continue to be unbounded iterates or bounded iterates with one species zero.

4.4 ANALYSIS OF SYSTEM (1-1-4) WITH LINEAR ATTRITION

We remove the bilinear attrition and source terms from system (1-1-4) to get

$$\begin{aligned}x_{n+1} &= A_1 x_n (1 - B_1 x_n) - D_1 y_n \\ y_{n+1} &= A_2 y_n (1 - B_2 y_n) - D_2 x_n\end{aligned}\tag{4-4-1}$$

Numerical analysis shows that this system is much more well-behaved than system (3-1-1). Specifically, we observed that for both large and small quadratic self-repression effects, system (3-3-1) displays positive, bounded iterates in both species for a considerable range of parameter values. Chaos and bifurcations from periodicity to fixed points to chaos were observed (see Figures 19, 20, and 21). As in the case of system (3-1-1) for large quadratic effects, bifurcations in both species were always seen to occur in phase.

We analyzed the effect of perturbing system (4-4-1) with low quadratic effects by adding a small amount of bilinear attrition in one or both species. In the cases observed, small bilinear effects had a strong effect on model dynamics (see Table 7). Only bilinear attrition comparable in size and smaller than the quadratic self-repression was seen to result in bounded iterates.

TABLE 6

The effect of small perturbations on equally configured forces in system (1-1-4). The unperturbed system has the parameter values: $A_1 = A_2 = 1.7$, $B_1 = B_2 = 0.2$, $C_1 = C_2 = 0.8$, $D_1 = D_2 = 0.5$, $E_1 = E_2 = 0$, and the initial conditions $x_0 = y_0 = 0.5$.

Case: Species	unperturbed		$B_1 = 0.201$		$C_1 = 0.801$		$D_1 = 0.501$		$A_1 = 1.701$	
	x	y	x	y	x	y	x	y	x	y
<u>Iterate</u>										
1	0.175	0.175	0.174	0.175	0.174	0.175	0.174	0.175	0.175	0.175
2	0.157	0.157	0.157	0.158	0.157	0.158	0.157	0.158	0.158	0.157
3	0.147	0.147	0.145	0.147	0.145	0.147	0.145	0.148	0.148	0.146
4	0.139	0.139	0.137	0.141	0.137	0.141	0.136	0.142	0.141	0.138
5	0.134	0.134	0.129	0.138	0.129	0.138	0.128	0.140	0.138	0.131
6	0.127	0.127	0.121	0.140	0.121	0.140	0.117	0.143	0.138	0.123
7	0.125	0.125	0.107	0.147	0.107	0.147	0.099	0.155	0.144	0.111
Steady State	Fixed point at $x = y = .117$		Unbounded		Unbounded		Unbounded		Unbounded	

4.5 CONCLUSIONS FOR THE ANALYSIS OF SYSTEM (1-1-4)

System (1-1-4) was found to generate steady-state solutions with both species positive, including fixed, periodic, and chaotic, solutions for both linear and bilinear attrition as long as quadratic self-repression is large compared to the bilinear attrition. System (1-1-4) continues to display such dynamics for small self-repression with linear attrition but not with bilinear attrition. Bilinear attrition combined with relatively small self-repression results in steady-state solutions with at least one species zero or in unbounded iterates.

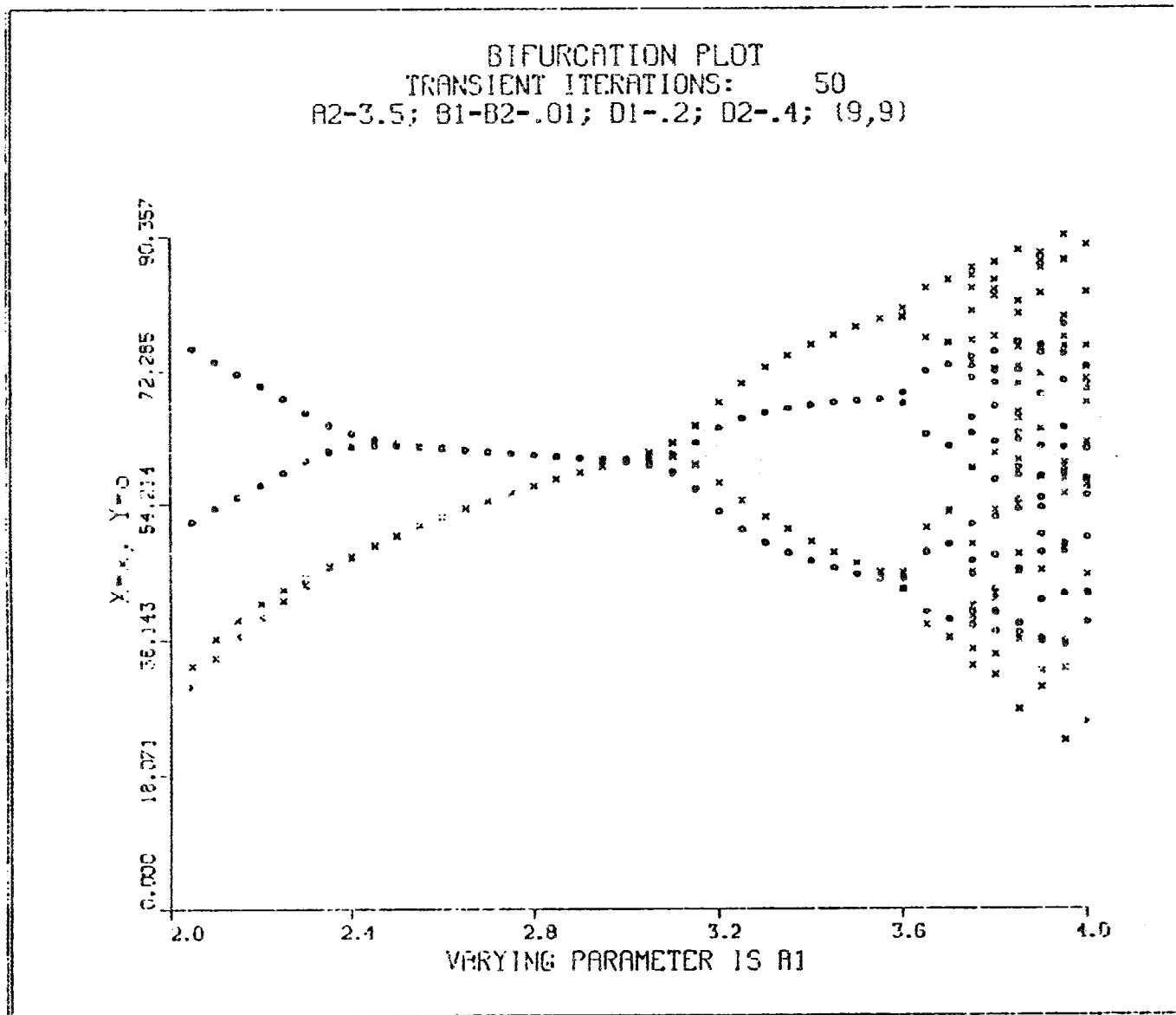


Figure 19. Bifurcation plot for system (1-1-4).

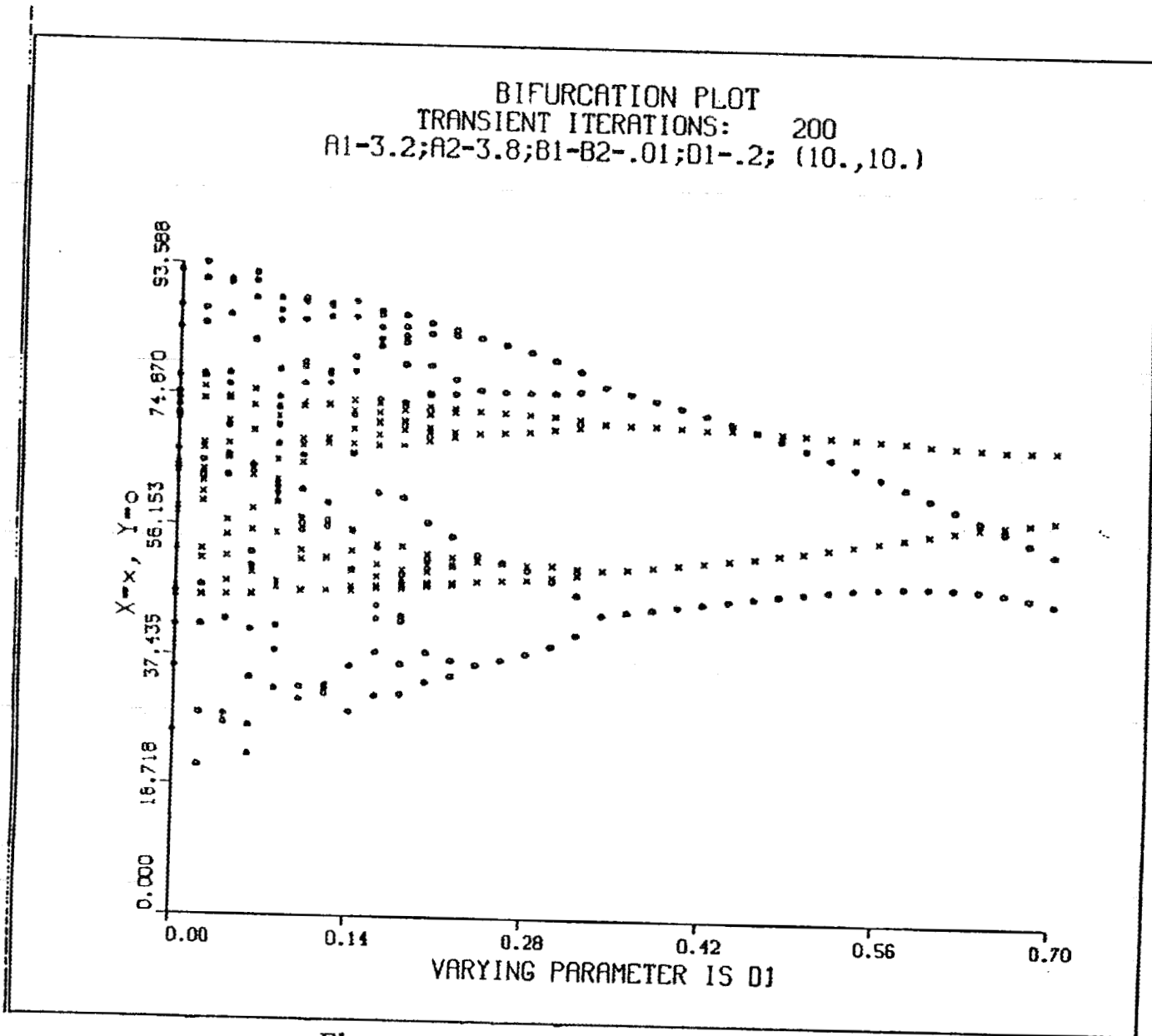


Figure 20. Bifurcation plot for system (1-1-4).

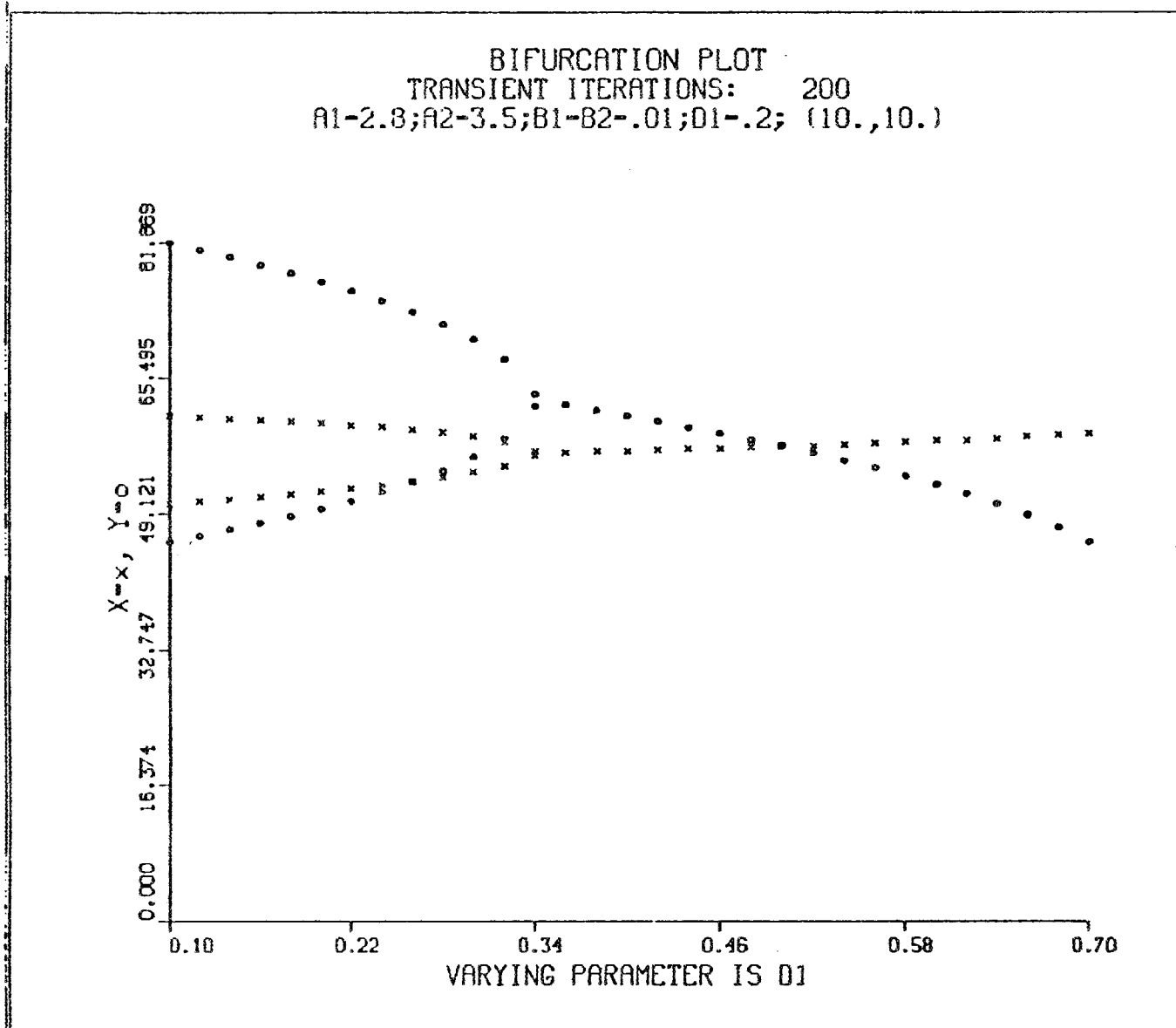


Figure 21. Bifurcation plot for system (1-1-4).

TABLE 7

The strong effect of addition of bilinear attrition has on a system with linear attrition.

System (1-1-4) with $A_1 = 2.0$, $A_2 = 2.05$, $B_1 = 0.01$, $B_2 = 0.014$, $D_1 = 0.2$, $D_2 = 0.16$, $x_0 = 0.6$, $y_0 = 0.6$.

Case: Species: Iteration	$C_1 = 0, C_2 = 0$		$C_1 = 0.002, C_2 = 0.001$		$C_1 = 0.02, C_2 = 0.01$	
	x	y	x	y	x	y
1	1.07	1.12	1.07	1.12	1.05	1.11
2	1.89	2.09	1.89	2.09	1.82	2.05
3	3.30	3.86	3.27	3.85	3.01	3.73
4	5.61	6.96	5.51	6.92	4.65	6.53
5	9.21	11.99	8.88	11.85	6.35	10.8
6	14.32	18.98	13.39	18.62	7.00	16.36
7	20.74	26.28	18.48	25.57	5.16	22.39
8	27.63	30.73	23.12	29.73	0.69	28.31
9	33.84	31.47	26.85	30.46	-5.07	34.52
10	38.48	30.67	29.92	29.84	-10.55	40.96
11	41.21	29.72	32.39	28.99	-14.23	46.37
12	42.51	28.98	34.24	28.20	-15.39	49.16
13	43.08	28.50	35.53	27.52	-15.08	49.39
14	43.34	28.22	36.39	26.99	-14.79	48.92
15	43.46	28.06	36.96	26.58	-14.79	48.80
16	43.53	27.97	37.35	26.28	-14.84	48.86
17	43.56	27.92	37.61	26.06	-14.85	48.89
18	43.58	27.89	37.79	25.90	-14.85	48.89
19	43.59	27.87	37.92	25.79	-14.85	48.89
20	43.60	27.86	38.01	25.70	-14.85	48.89

5. NUMERICAL ANALYSIS OF SYSTEM (1-1-1)

5.1 INTRODUCTION

The results of further numerical analyses of system (1-1-1) are presented in the following sections. In Section 5.2, the computer program used in the analysis is described. Section 5.3 discusses further results for the one species case of system (1-1-1) used to test program correctness. Section 5.4 compares the dynamics of the space-independent system (1-1-4) with system (1-1-1).

5.2 DESCRIPTIONS OF THE PROGRAMS

System (1-1-1) was numerically analyzed with a computer program called MAP1V2, written in double-precision VAX FORTRAN.⁸ It was based on a previous program written by S. de Rada¹³ called MAP1. A sister program of MAPV2 was written, namely MAP1V1 which is a four-species-capable version of MAP1V2. While all analyses that can be run on MAP1V2 can, of course, also be run on MAP1V1, the less complex MAP1V2 can run two species simulations faster than the more complex MAP1V1.

Both programs require a user edited data file and function file. Through the data file the user directs how the time-space mesh shall be configured, supplies the values of the coefficients, initial conditions and boundary conditions as needed, identifies the parameter to be varied and supplies bounds, and directs the formatting of the output. The function file describes the functional dependence on distance of the diffusion, convection, initial conditions, etc., for each species as stated in system (1-1-1).

The output of MAP1V1 and MAP1V2 consists of a file containing the results of the simulation and an optional graphics file generated using the DISSPLA⁹ graphics subroutine library.

Both programs are menu driven by Digital Command Language¹² command files.

5.3 ONE-SPECIES DYNAMICS

Results given by MAP1V2 were compared with those found by Mitchell and Bruch¹⁴ as well as with those found by de Rada¹¹ to prove correctness of the program. Figure 22 was generated by system (1-1-1) by varying the diffusion with $a_{111} = 20$, $b_{11} = -12$, and all other coefficients zero. Figure 23 shows the similar effect of varying convection for small diffusion. Here we took $a_{111} = 20$ and $b_{11} = -12$, $D = 0.1$, and all other coefficients zero. For Figure 24, system (1-1-1) was configured identically as for Figure 23 except D was taken as 0.35. Comparing Figures 23 and 24, we see that bifurcations and chaos occur for smaller values of convection as diffusion is increased. This effect is similar with the one reported in Reference 4 where it was found that the onset of bifurcations and chaos occurs for

smaller values of diffusion as convection is increased. These two findings have the potential for important practical applications.

5.4 A COMPARISON OF SYSTEM (1-1-4) AND SYSTEM (1-1-1) DYNAMICS

We now briefly study how the dynamics described in Part 2 for system (1-1-1) change as a spatial dimension and the effects of diffusion and convection are added. We first observed the effect of adding diffusion to bilinear attrition and large self-repression cases. Figures 25, 26, and 27 show the results for such a case. The addition of diffusion with homogeneous Neumann boundary conditions has not been seen to drastically alter the behavior of bilinear attrition, high self-repression cases. On the other hand, the addition of diffusion with Dirichlet boundary conditions can have a pronounced effect. Figures 26 and 28 were generated by the same system except in Figure 28, Dirichlet instead of Neumann boundary conditions were used, forcing the iterates into chaos for low values of the local bilinear attrition. The different effects of Neumann and Dirichlet boundary condition were also seen in simulations of system (1-1-1) for local linear attrition with low self-repression. The specification of Dirichlet boundary conditions were seen in cases to lead to unbounded iterates at and near the boundaries of the mesh. By choosing homogeneous Neumann boundary conditions, we eliminated this problem.

Local bilinear attrition with small self-repression was again seen to produce solutions with either one species zero or to result in unboundedness, even in the presence of diffusion.

The effects of spatially-dependent nonlocal interaction were next examined. The nonlocal attrition function used in the studies was

$$\eta e^{-(0.01)|m-l|} \quad (3-4-1)$$

where η is a constant.

Cases were simulated with both species initially uniformly distributed, either over the entire mesh or each over a region at the ends of the mesh. For both species initially uniformly distributed, either over the entire mesh or each over a region at the ends of the mesh. For both types of distribution, nonlocal bilinear attrition with low self-repression displayed essentially the same dynamics discussed in Section 2, even in the presence of diffusion with Neumann boundary conditions. For example, Figure 29 shows a low self-repression, nonlocal bilinear attrition simulation. Figure 30 shows the same simulation with the addition of diffusion in u_1 with Neumann boundary conditions.

For a separated initial distribution, nonlocal linear attrition and diffusion, we have observed the iterates at the nodes which represent the fronts of the two species to become unbounded. This "fringe-effect" occurs because the densities at these nodes are originally zero, then due to diffusion become small and positive, too small to sustain the effects of the nonlocal linear attrition. Thus, these iterates rapidly become negative and unbounded.

5.5 CONCLUSIONS

The purpose of the brief discussion above was to point out that the dynamics studies in Sections 5.2 and 5.3 for system (1-1-4) are relevant to the dynamics of

MAP1:Version 2. 7-25-89. 13:22
MMAX-200;PLOT# 0; Mitchell & Bruch Case
50 TRANSIENTS, 18 PLOTTED

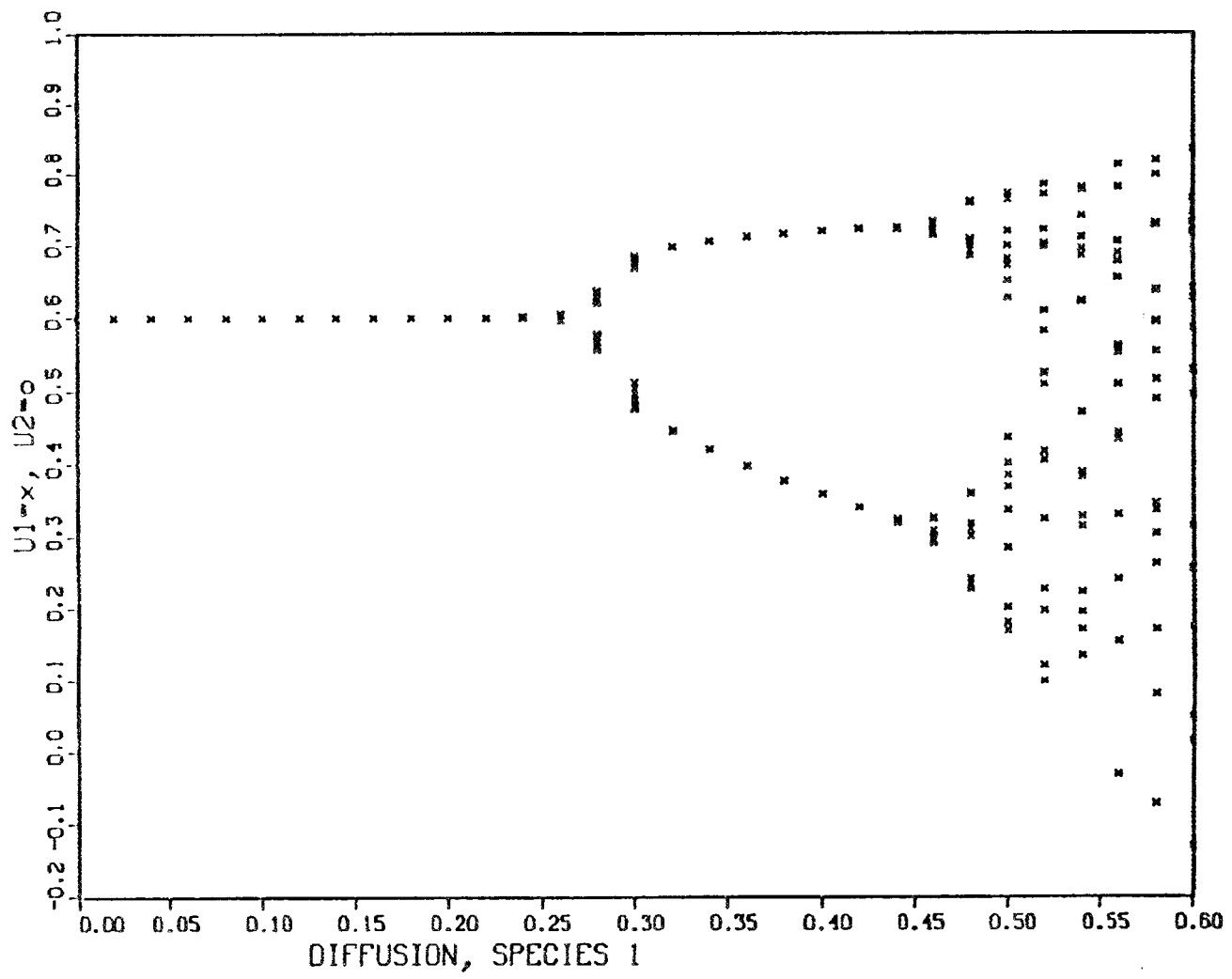


Figure 22. Bifurcation plot for system (1-1-1). This case is described in Reference 11.

MAP1:Version 2. 7-25-89. 12:02
MAYX-40;PLOT# 0; 1 species; diff.-. 1
40 TRANSIENTS, 10 PLOTTED

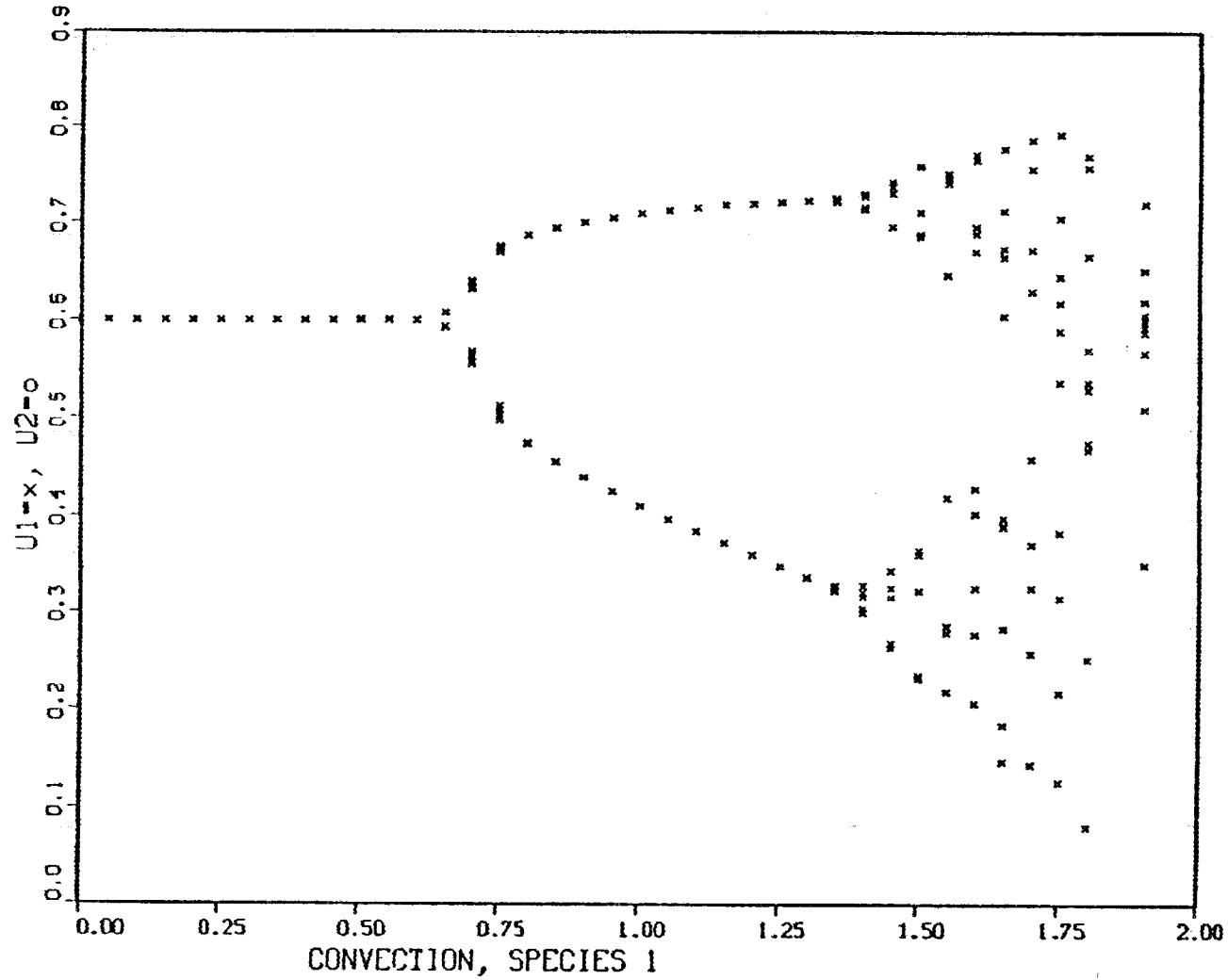


Figure 23. Bifurcation plot for system (1-1-1). This case is the same as the previous except diffusion is held constant at $D = 0.1$ and convection is allowed to vary.

MAP1:Version 2. 7-26-89. 03:40
MITCHELL & BRUCH CASE, D=0.35
MMAX=50;PLOT @ 0; 100 TRNS,18 POINTS

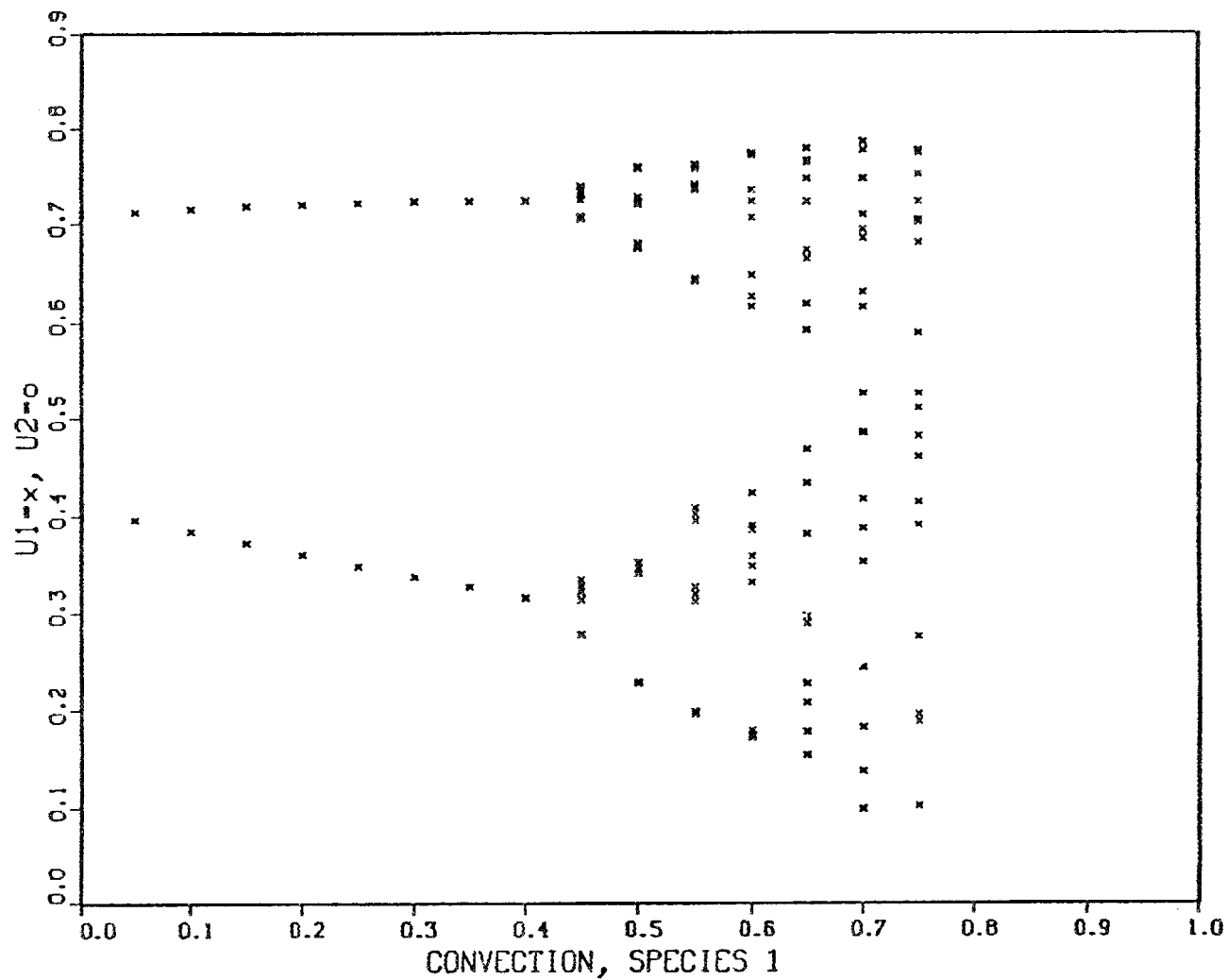


Figure 24. Bifurcation plot for system (1-1-1). This case is the same as the previous except diffusion is held constant at $D = 0.35$ and convection is allowed to vary.

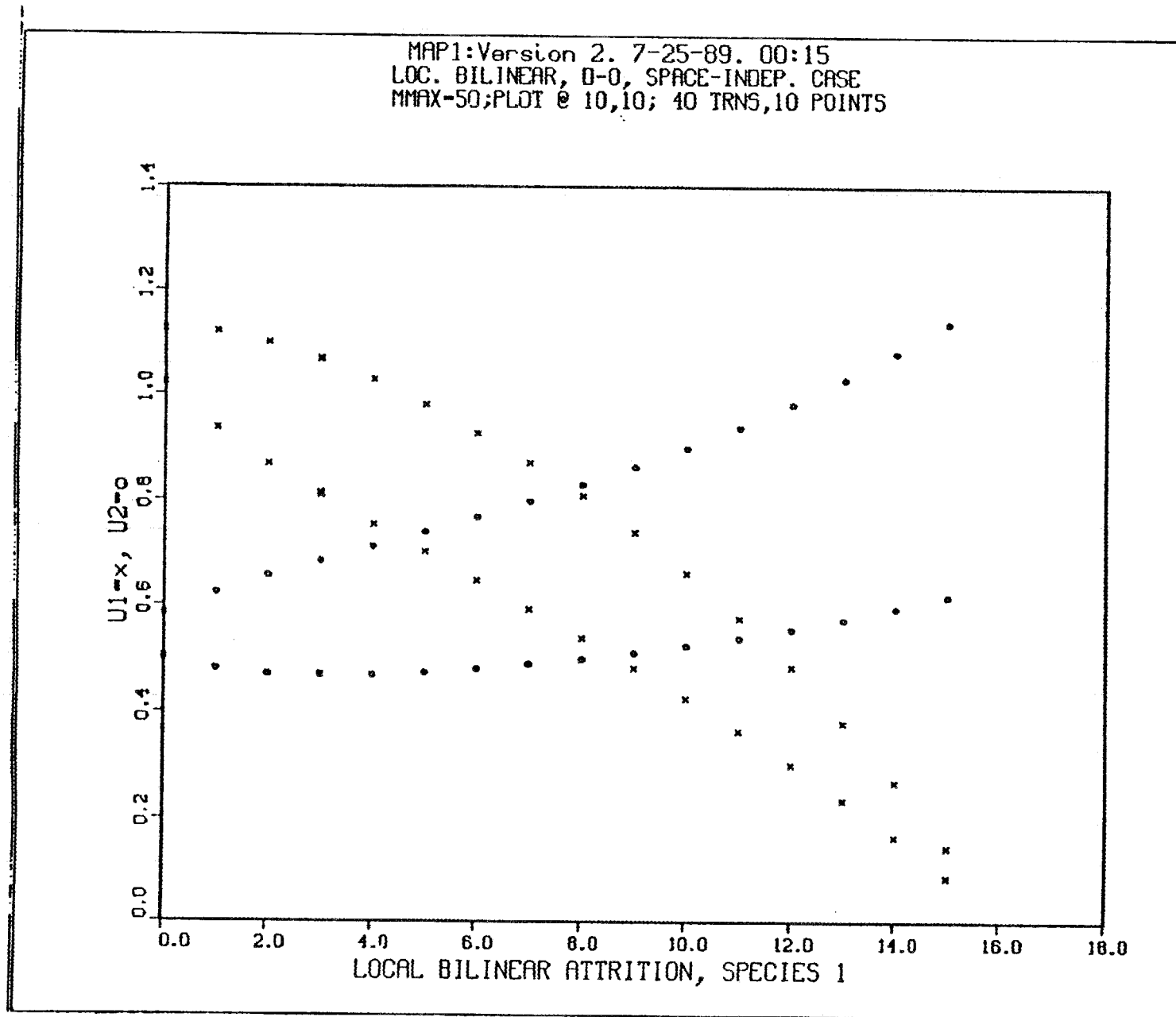


Figure 25. Bifurcation plot for system (1-1-1). This figure and the following two show that the addition of diffusion with Neumann boundary conditions has little effect on the system's dynamics.

MAP1:Version 2. 7-25-89. 00:02
LOC. BILINEAR, D- 2, NEUMANN B.C.
MMAX-50;PLOT @ 10,10; 40 TRNS,10 POINTS

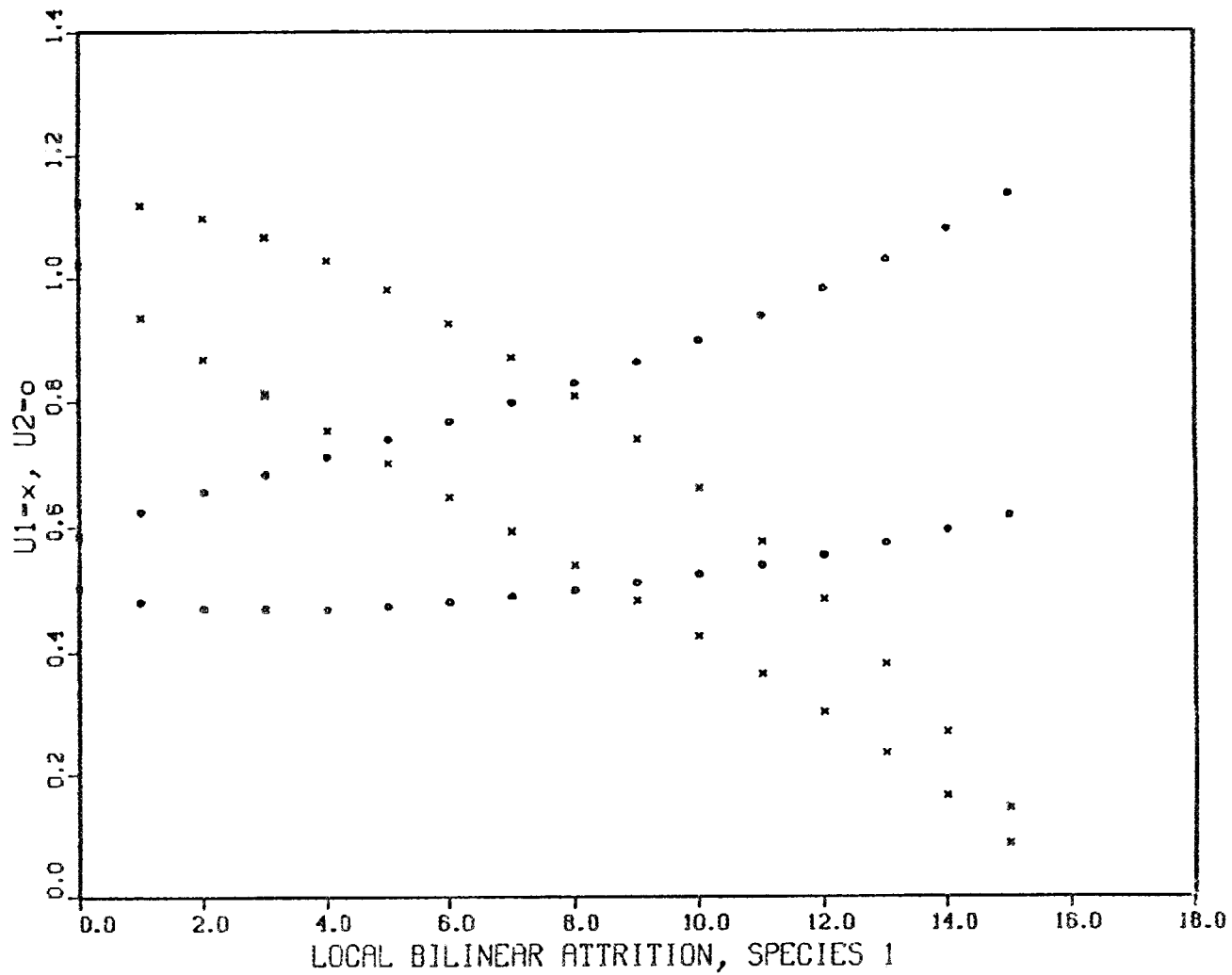


Figure 26. Bifurcation plot for system (1-1-1).

MAP1:Version 2. 7-25-89. 00:12
LOC. BILINEAR, D-.4, NEUMANN B.C.
MMAX-50;PLOT @ 10,10; 40 TRNS,10 POINTS

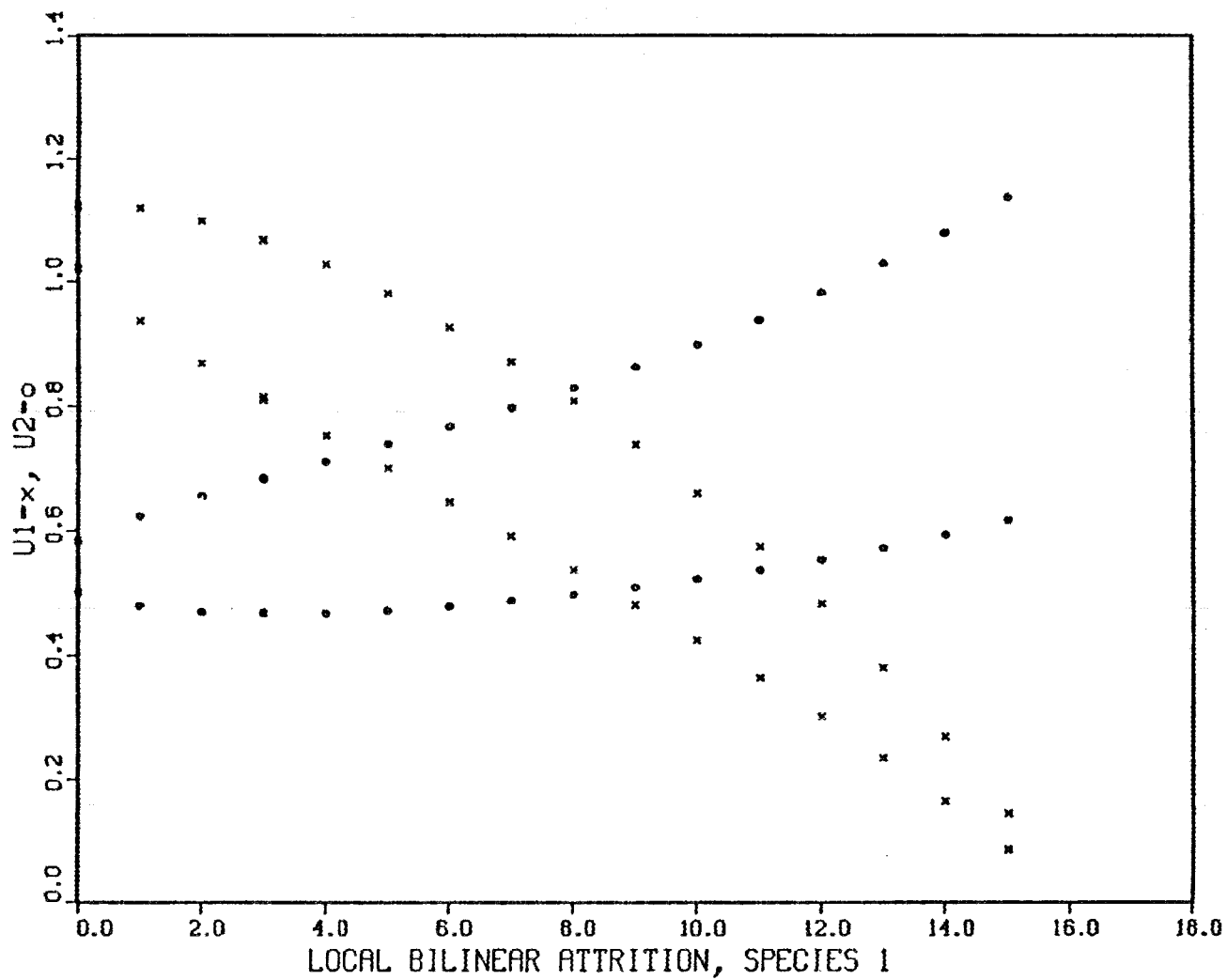


Figure 27. Bifurcation plot for system (1-1-1).

MAP1:Version 2. 7-26-89. 00:40
LOC. BILINEAR, D-.2, DIRICHLET B.C.
MMAX-50;PLOT @ 10,10; 40 TRNS,10 POINTS

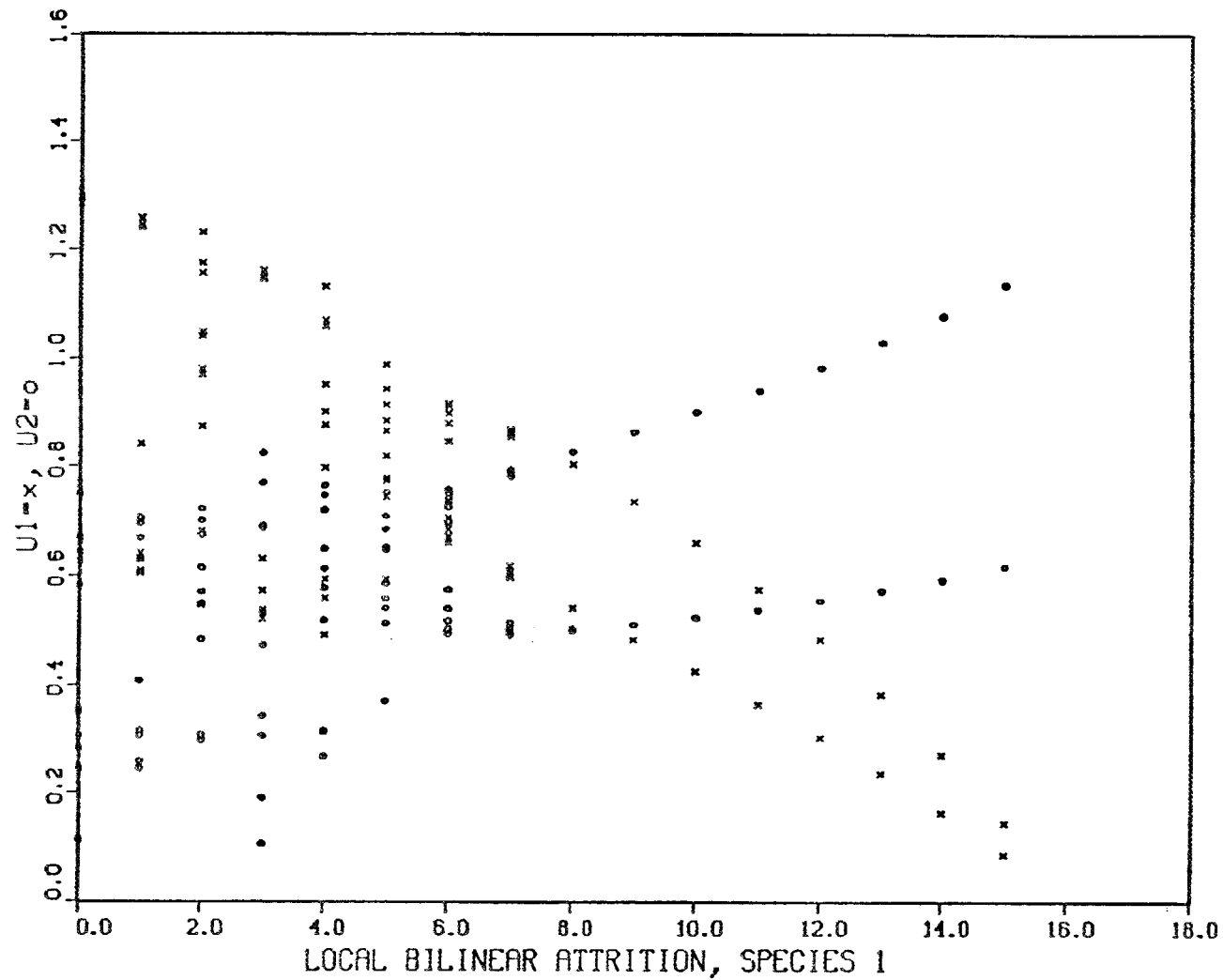


Figure 28. Bifurcation plot for system (1-1-1). Here, Dirichlet boundary conditions ($u_1, u_2 = 10$ at both boundaries) were used, substantially affecting the dynamics.

MAP1:Version 2. 7-26-89. 01:20
NLOC. BILINEAR, D-0, MAP CASE
MMAX-50;PLOT @ 10,10; 40 TRNS,10 POINTS

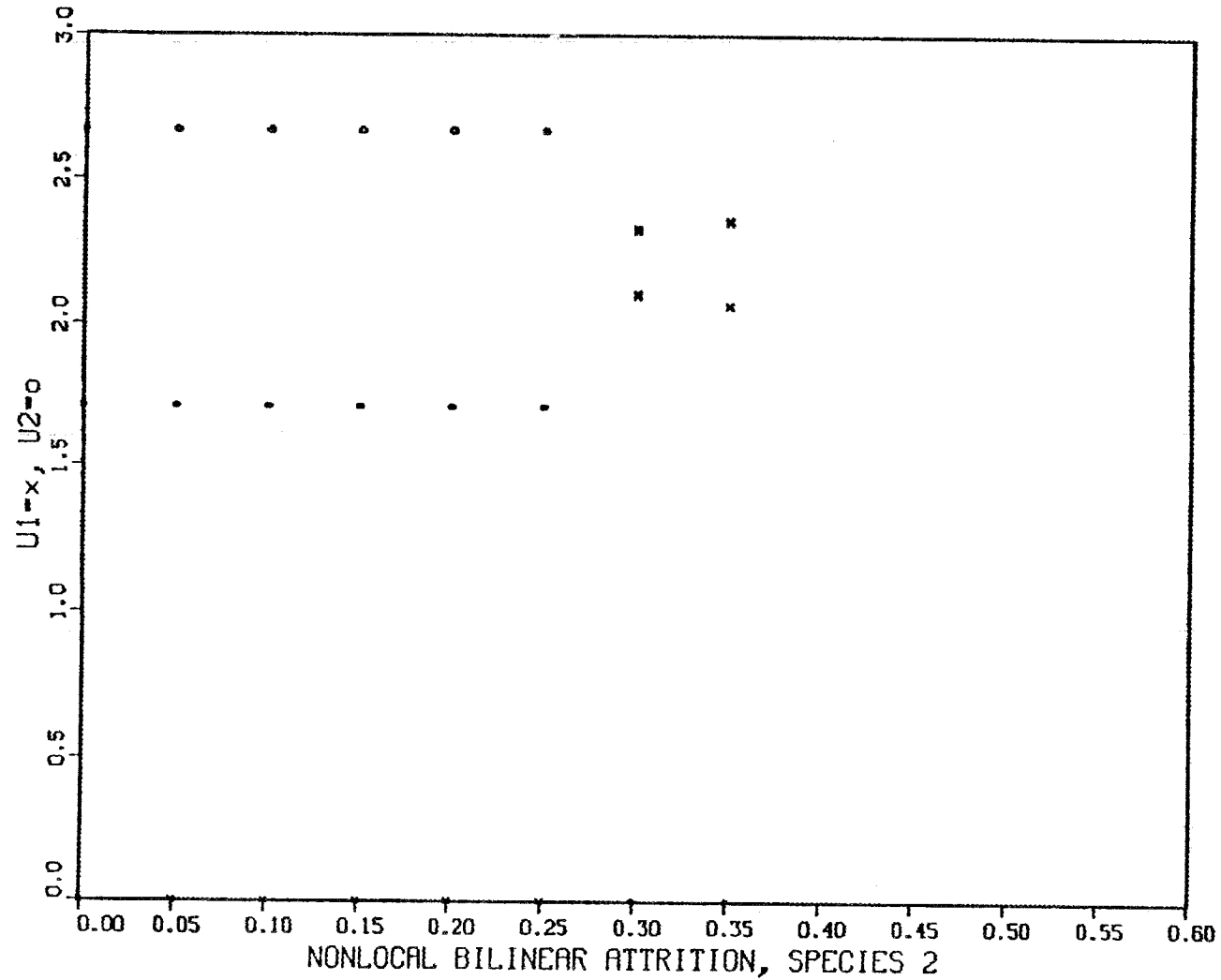


Figure 29. Bifurcation plot for system (1-1-1). Note that in this figure and the next, one species always asymptotically approaches zero.

MPI:Version 2. 7-26-89. 01:30
NLOC. BILINEAR, D1-.3, D2-0, NEUMANN
MMAX-50;PLOT @ 10,10; 40 TRNS,10 POINTS

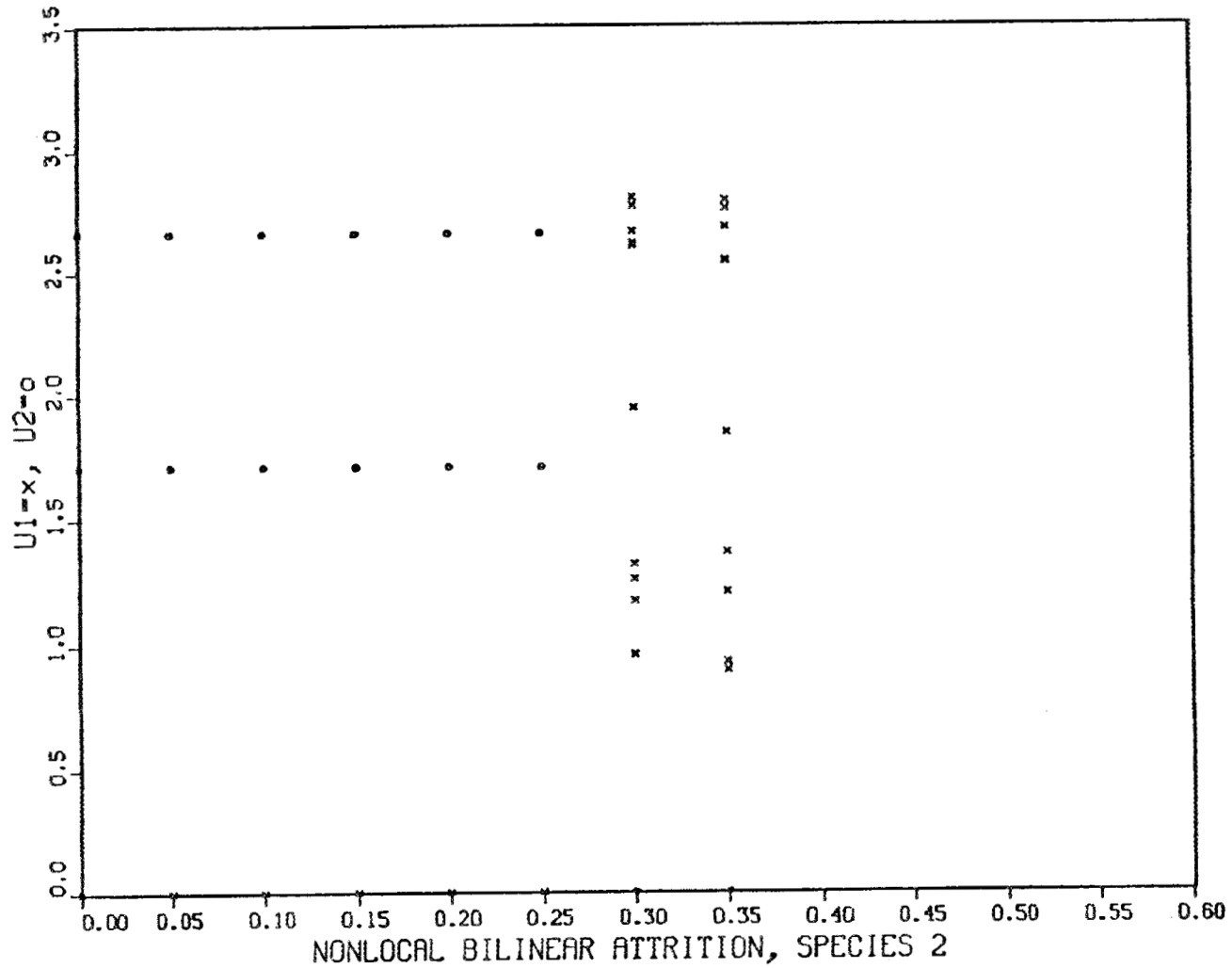


Figure 30. Bifurcation plot for system (1-1-1). Again, one species always asymptotically approaches zero.

system (1-1-1). Also, new problems that occur for system (1-1-1), such as boundary condition specification and "fringe-effects," were highlighted. Future studies may show the "fringe-effects" can be avoided by appropriately selecting nonlocal linear attrition functions. Furthermore, it remains to be seen whether the pathological dynamics that occur for bilinear attrition and low self-repression in system (1-1-4) can be controlled with judicious and physically acceptable choices of parameters, boundary conditions, nonlinearities, etc., in system (1-1-1).

6. CALCULATION OF THE CORRELATION DIMENSION OF THE CHAOTIC ATTRACTOR

6.1 INTRODUCTION

The two species "bilogistic" system

$$\begin{aligned} X_{n+1} &= A_1 X_n (1 - (1 - A)X - AY) \\ Y_{n+1} &= A_2 Y_n (1 - (1 - A)Y - AX) \end{aligned} \quad (6-1-1)$$

harbors a chaotic attractor for $A_1 = 3.87$, $A_2 = 3.8$, and $A = 0.2$, similar to the one shown in Figure 10. In this chapter we describe our calculations of the correlation dimension, ν , of this attractor. The correlation dimension has been shown to be a lower bound on the Hausdorff dimension.¹⁵⁻¹⁷ Yet, it is much simpler and less costly to calculate than the Hausdorff dimension and may even be more meaningful.^{15,16}

6.2 ESTIMATION OF THE CORRELATION DIMENSION

The correlation dimension of the attractor was calculated using the method introduced by Grassberger and Procaccia.^{15,16} A total of m vectors in p -dimensional iterate space are formed from the iterates of a single species (observable):

$$\bar{V}_i = (X_i, X_{i+1}, \dots, X_{i+p-1}), \quad i = 1, 2, \dots, m, \quad (6-2-1)$$

The spatial correlation of these points is found by applying the correlation integral¹⁷:

$$C(r) = \lim_{m \rightarrow \infty} \frac{1}{m^2} \sum_{i,j=1}^m H(r - |x_i - x_j|) \quad (6-2-2)$$

where H is the heavyside function defined by $H(x) = 1$ for x positive, 0 otherwise.¹⁷ The sum above can be viewed as placing at every point on the attractor, now embedded in a p -dimensional iterate-space, p -dimensional hyperspheres of radii r and summing the points within the hyperspheres.

It has been shown¹⁵⁻¹⁷ that the correlation integral behaves as a power of r for small r :

$$C(r) \sim r^\nu \quad (6-2-3)$$

where ν is the correlation exponent, or dimension, which means the logarithm of $C(r)$ has a linear dependence on the logarithm of r with a slope of ν . Thus, ν can be determined by choosing a sample of hypersphere radii, calculating their corresponding correlation integrals and performing a regression analysis of the results to estimate ν .

The values of p , m , and r must be judiciously chosen. The dimension of the iterate space must be greater than the dimension of the attractor. Grassberger and Procaccia advocate choosing p larger than strictly necessary in order to eliminate systematic errors. They also caution that increasing p increases statistical errors, so a compromise must be reached. If the iterate comes from a measurement instead

of a model, Bergé et al.¹⁷ advocate calculation of ν for a range of increasing p ; if ν continues to increase with p , then the signal is white noise.

The values found for the correlation integrals will, of course, depend on the number of vectors, m , that are compared. Although Grassberger and Procaccia^{1,2} have used $\sim 20,000$ points in their calculations, they have stated that convergence usually occurs with a few thousand points. Furthermore, they have stated convergence with fewer points occurs faster for larger p , and it is generally more important to embed the attractor in a larger dimensional phase space than to increase the number of points. It has been suggested¹⁷ that ~ 100 points is sufficient for a reasonable estimate of ν if a range of iterate-space dimensions are used.

The values of the hypersphere radii must be chosen with reference to the size of the attractor in phase space. If r is too small, statistical errors will dominate,¹⁷ while if r is too larger, resolution will be insufficient and the sum in (6-2-2) approaches unity.

A double precision VAX FORTRAN⁸ computer program, SATRCT, was written to implement the method described. The program takes, as input, a file containing the iterates of the observed variable and a file which specifies the values of m , p , the hypersphere radii, and other user options. The program outputs the calculated correlation integral for each r . It also outputs the sample regression coefficient for the logarithms of the correlation integrals versus the logarithms of the hypersphere radii obtained by a Gaussian least-squares fit.¹⁸ The sample regression coefficient serves as an estimate of ν .

6.3 RESULTS

The program was tested on the Henon Map and the results compared well with the known Hausdorff dimension and other published results (see Table 8).

The preliminary results for the system (6-1-1) are shown in Table 9. In Figure 31, the points formed by the logs of the correlation integral versus the logs of their corresponding hypersphere radii for $m = 500$ and a range of embedding dimensions are fit with a least-squares regression line. This line represents an estimate of the correlation dimension.

In order to determine the correlation integral with certainty, a much larger m would be needed.^{15,16} Because of the large CPU time requirement, this becomes quite expensive. In order to reduce CPU cost and obtain confidence limits on ν , we are now conducting a statistical investigation of the correlation integral as described below.

6.4 A STATISTICAL ANALYSIS

We are using SAS¹⁹ to model the behavior of the correlation integral as a function of the number of iterate-space points for a given hypersphere radius. Such a model may yield a good estimate of the asymptotic value of the correlation integral for a smaller number of iterate-space points than required by current methods. It also may allow an analysis of the errors associated with the calculation of the correlation integrals and the correlation dimension.

However, a problem has arisen in that the errors are highly autocorrelated. Autocorrelation in the results means that the error estimates returned by SAS are questionable. Current efforts are directed at surmounting this problem.

BILOGISTIC MAP: $\text{LOG}(C(r))$ vs. $\text{LOG}(r)$
USING 500 POINTS

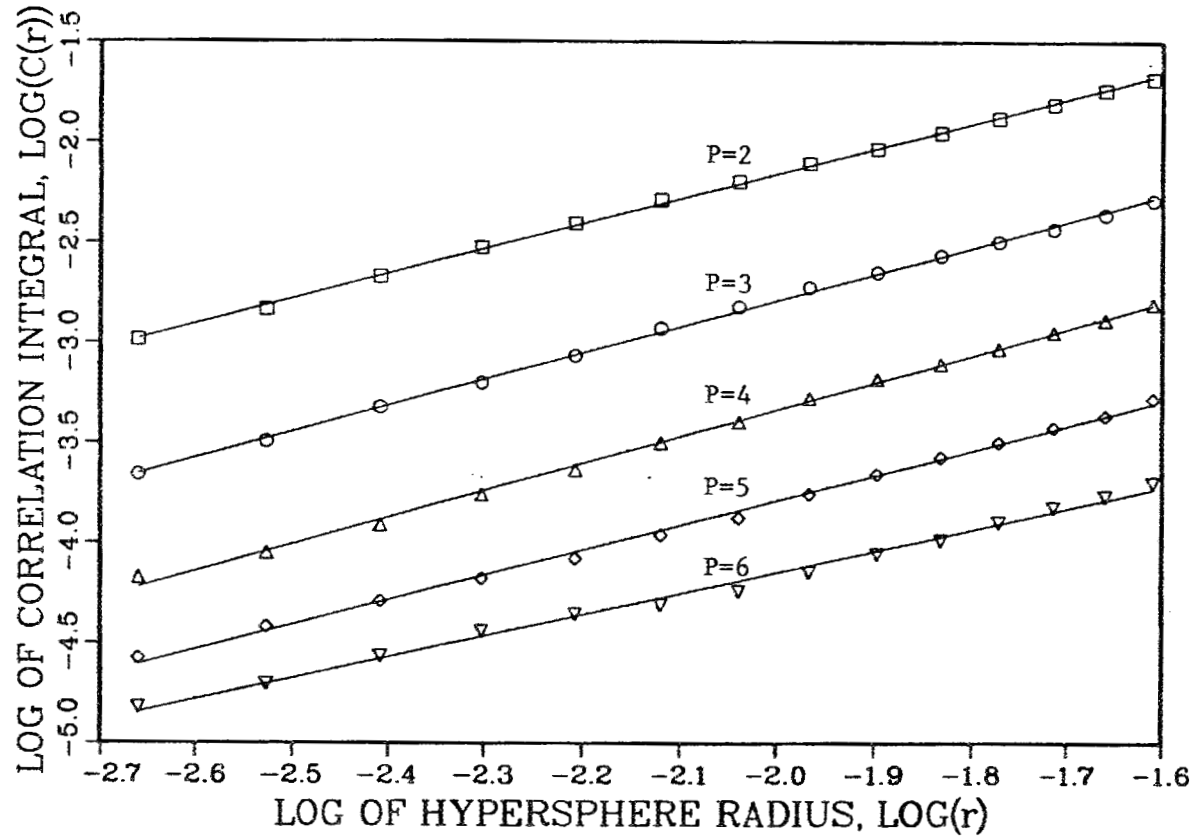


Figure 31. Plot of the correlation integral as a function of the hypersphere radius (log scale).

Table 8. Results for the Henon Attractor

Embedding Dimension Number of Points	2	3	4	5	6
100	0.94212	0.81591	0.55757	0.39722	0.33508
200	1.1425	1.0389	0.77740	0.62302	0.50621
500	1.1835	1.2010	1.0402	0.9421	0.8608
2000	1.1802	1.2574	—	—	—

Table 9. Results for the Bilogistic Attractor

Embedding Dimension Number of Points	2	3	4	5	6
100	1.2188	1.1676	1.0096	0.86658	0.63170
200	1.2458	1.3087	1.3428	1.2382	1.0570
500	1.2453	1.3384	1.3926	1.4022	1.3231
2000	1.2261	1.3605	—	—	—

APPENDIX 1

MACSYMA OUTPUT for the map (2-1-1)

The results on page 62 are the fixed and period-two points for the system Eqs. (2-1-1) with A_1 not equal to A_2 (in the MACSYMA output, $A1 = A_1$ and $A2 = A_2$). Note that MACSYMA does not find the parameterized family that exists for $A_1 = A_2$. This solution is found by MACSYMA when A_1 is set equal to A_2 in Eqs. (2-1-1) as the results on pages 63 and 64 show.

\$ This is Macsyma 412.61 for DEC VAX 8650 Series Computers.
 Copyright (c) 1982 Massachusetts Institute of Technology.
 All Rights Reserved.
 Enhancements (c) 1982, 1988 Symbolics, Inc. All Rights Reserved.
 Type "DESCRIBE(TRADE_SECRET);" to see important legal notices.
 Type "HELP();" for more information.

Checking password file: S1:[MACSYMA_412.SYSTEM]PASSWD-STCVAX8600-412.TEXT

Init File Not Found: U2:[DFN]macsyma-init.mac

(C1)

(C2)

(C3)

(C4)

(D4)

The equations being investigated are:

(C5)

(D5)

(C6)

(D6)

(C7)

(C8)

$$F1(X, Y) := A1 X (1 - \frac{X}{2} - \frac{Y}{2})$$

$$F2(X, Y) := A2 Y (1 - \frac{Y}{2} - \frac{X}{2})$$

The Period 1 Roots Are:

$$[[X = 0, Y = 0], [X = \frac{2 A1 - 2}{A1}, Y = 0], [X = 0, Y = \frac{2 A2 - 2}{A2}]]$$

The Period 2 Roots Are:

$$[[X = 0, Y = 0], [X = \frac{\text{SQRT}(A1^2 - 2 A1 - 3) - A1 - 1}{A1}, Y = 0],$$

$$[X = \frac{\text{SQRT}(A1^2 - 2 A1 - 3) + A1 + 1}{A1}, Y = 0], [X = \frac{2 A1 - 2}{A1}, Y = 0],$$

$$[X = 0, Y = \frac{\text{SQRT}(A2^2 - 2 A2 - 3) - A2 - 1}{A2}],$$

$$[X = 0, Y = \frac{\text{SQRT}(A2^2 - 2 A2 - 3) + A2 + 1}{A2}], [X = 0, Y = \frac{2 A2 - 2}{A2}]]$$

(C9)

This is Macsyma 412.61 for DEC VAX 8650 Series Computers.

Copyright (c) 1982 Massachusetts Institute of Technology.

All Rights Reserved.

Enhancements (c) 1982, 1988 Symbolics, Inc. All Rights Reserved.

Type "DESCRIBE(TRADE_SECRET);" to see important legal notices.

Type "HELP();" for more information.

Checking password file: S1:[MACSYMA_412.SYSTEM]PASSWD-STCVAX8600-412.TEXT

Init File Not Found: U2:[DFN]macsyma-init.mac

(C1)

(C2)

(C3)

(C4)

(D4)

The equations being investigated are:

(C5)

(D5)

$$F1(X, Y) := A1 X (1 - \frac{X}{2} - \frac{Y}{2})$$

(C6)

(C7)

(C8)

The Period 1 Roots Are:

$$[[X = \%R1, Y = -\frac{\%R1 A1 - 2 A1 + 2}{A1}], [X = 0, Y = 0], [X = \frac{A1 - 1}{A1}, Y = \frac{A1 - 1}{A1}]]$$

The Period 2 Roots Are:

$$[[X = \%R2, Y = -\frac{\%R2 A1 - 2 A1 + 2}{A1}], [X = \%R3,$$

$$Y = \frac{\text{SQRT}(A1^2 - 2 A1 - 3) - \%R3 A1 + A1 + 1}{A1}],$$

$$X = \%R4, Y = \frac{\text{SQRT}(A1^2 - 2 A1 - 3) + \%R4 A1 - A1 - 1}{A1}], [X = 0, Y = 0],$$

$$X = -\frac{\text{SQRT}(A1^2 - 2 A1 - 3) - A1 - 1}{4 A1}, Y =$$

$$\frac{3 \text{SQRT}(A1 - 3) \text{SQRT}(A1 + 1) - 3 A1 - 3}{4 A1}],$$

$$[X = \frac{\text{SQRT}(A_1^2 - 2 A_1 - 3) + A_1 + 1}{4 A_1}, Y = \frac{3 \text{SQRT}(A_1 - 3) \text{SQRT}(A_1 + 1) + 3 A_1 + 3}{4 A_1}], [X = \frac{A_1 - 1}{2 A_1}, Y = \frac{3 A_1 - 3}{2 A_1}]$$

(C9)

REFERENCES

1. Y. Y. Azmy and V. Protopopescu, *Two Dimensional Maps Generated by Competitive Systems*, ORNL/TM-11026, Oak Ridge National Laboratory, February 1989.
2. V. Protopopescu, R. T. Santoro, and J. Dockery, "Combat Modeling with Partial Differential Equations," *European Journal of Operations Research* **38**, 178 (1989).
3. R. T. Santoro, P. Rusu, and J. M. Barnes, *Mathematical Descriptions of Offensive Combat Maneuvers*, ORNL/TM-11000, Oak Ridge National Laboratory, January 1989.
4. M. Braun, *Differential Equations and Their Applications*, Springer-Verlag, Inc., New York, New York, 1983.
5. N. S. Goel, S. C. Meritra, and E. W. Montroll, "On the Volterra and Other Non-Linear Models of Interacting Populations," *Reviews of Modern Physics* **43**, 231 (1971).
6. MAP, by Sergio de Rada.
7. DPMAP, by David F. Scollan.
8. VAX FORTRAN Language Reference Manual (June 1988), Digital Equipment Corporation, Maynard, Massachusetts.
9. DISSPLA User's Manual, Version 10.0, Integrated Software Systems Corporation, San Diego, California 92121.
10. MACSYMA Reference Manual, Version 13 (November 1988), Symbolics, Inc., Burlington, Massachusetts 01803.
11. S. de Rada, "Numerical Analysis of Competitive Systems," unpublished report, Oak Ridge National Laboratory, December 1988.
12. Guide to Using DCL and Command Procedures on VAX/VMS (September 1984), Digital Equipment Corporation, Maynard, Massachusetts.

13. MAP1, by Sergio de Rada.
14. A. R. Mitchell and J. C. Bruch, "A Numerical Study of Chaos in a Reaction-Diffusion Equation," *Numerical Methods for Partial Differential Equations* **1**, 13 (1985).
15. P. Grassberger and I. Procaccia, "Measuring the Strangeness of Strange Attractors," *Physica* **9D**, 189-208 (1983).
16. P. Grassberger and I. Procaccia, "Characterization of Strange Attractors," *Physical Review Letters*, Vol. 50, No. 5 (1983).
17. P. Bergé, Y. Pomeau, C. Yidal, *Order Within Chaos*, John Wiley & Sons, New York (1984).
18. E. Kreyszig, *Advanced Engineering Mathematics*, John Wiley & Sons, Inc., New York (1983).
19. *SAS User's Guide: Basics and SAS: User's Guide: Statistics* (1982), SAS Institute, Box 8000, Cary, North Carolina 27511.

INTERNAL DISTRIBUTION

- | | |
|------------------------|-----------------------------------------|
| 1. B. R. Appleton | 20. A. Zucker |
| 2-6. Y. Y. Azmy | 21. EPMD Reports Office |
| 7. T. J. Burns | 22-23. Laboratory Records
Department |
| 8. J. C. Culioli | 24. Laboratory Records,
ORNL-RC |
| 9. C. M. Haaland | 25. Document Reference
Section |
| 10. D. T. Ingersoll | 26. Central Research Library |
| 11. J. O. Johnson | 27. ORNL Patent Section |
| 12. F. C. Maienschein | |
| 13. J. R. Merriman | |
| 14-18. V. Protopopescu | |
| 19. R. T. Santoro | |

EXTERNAL DISTRIBUTION

28. David Baker, U. S. Army Materiel Systems Analysis Activity, UK RARDE, Aberdeen Proving Grounds, Maryland 21005
29. John Dockery, Office of the Joint Chiefs of Staff, J6F, Pentagon, Washington, D.C. 20301
30. J. J. Dorning, Department of Nuclear Engineering and Engineering Physics, Thornton Hall, University of Virginia, Charlottesville, Virginia 22901
31. R. M. Haralick, Department of Electrical Engineering, University of Washington, Seattle, Washington 98195
32. Robert L. Helmbold, Concepts Analysis Agency, 8120 Woodmont Avenue, Bethesda, Maryland 20814
33. Morton A. Hirschberg, U.S. Army Ballistics Research Laboratory, Aberdeen Proving Grounds, Maryland 21005
34. Richard Kaste, U.S. Army Ballistics Research Laboratory, Aberdeen Proving Grounds, Maryland 21005
35. Joe Lacetera, U.S. Army Laboratory Command, ATTN: AMCLD-PA, 2800 Powder Mill Road, Adelphi, Maryland 20783-1145
36. James E. Leiss, 13013 Chestnut Oak Drive, Gaithersburg, Maryland 20878
37. Robert McQuie, Concepts Analysis Agency, 8120 Woodmont Avenue, Bethesda, Maryland 20814
38. Neville Moray, Department of Mechanical and Industrial Engineering, University of Illinois, 1206 West Green Street, Urbana, Illinois 61801
39. Bob Orlov, Concepts Analysis Agency, 8120 Woodmont Avenue, Bethesda, Maryland 20814
40. Harry Peaker, U. S. Army Materiel Systems Analysis Activity, Aberdeen Proving Grounds, Maryland 21005
41. Richard Sandmeyer, Director USAMSAA, Army Materiel Systems Analysis Activity, AMKSY-CC, Aberdeen Proving Grounds, Maryland 21005-5071
- 42-46. David F. Scollan, 628 Leon Drive, Endicott, New York 13760
47. Hugh Thomas, Concepts Analysis Agency, 8120 Woodmont Avenue, Bethesda, Maryland 20814

48. E. B. Vandiver, III, Director, Concepts Analysis Agency, 8120 Woodmont Avenue, Bethesda, Maryland 20814
49. Sally Van Nostrand, U.S. Army Laboratory Command, 2800 Powder Mill Road, Adelphi, Maryland 20783-1145
50. Joseph Wald, U.S. Army Ballistics Research Laboratory, Aberdeen Proving Grounds, Maryland 21005
51. Mary F. Wheeler, Mathematics Department, University of Houston, 4800 Calhoun, Houston, Texas 77204-3476
52. Howard Whitley, Concepts Analysis Agency, 8120 Woodmont Avenue, Bethesda, Maryland 20814
53. A. E. R. Woodcock, Synectics Corporation, 10400 Eaton Place, Suite 200, Fairfax, Virginia 22030
54. Office of the Assistant Manager for Energy Research and Development, Department of Energy, Oak Ridge Operations, P.O. Box 2001, Oak Ridge, TN 37831
- 55-64. Office of Scientific and Technical Information, P.O. Box 62, Oak Ridge, Tennessee 37830